

# Stability of alkalinity in Ocean Alkalinity Enhancement (OAE) approaches - consequences for durability of CO<sub>2</sub> storage

Jens Hartmann<sup>1)\*</sup>, Niels Suitner<sup>1)\*</sup>, Carl Lim<sup>2)</sup>, Julieta Schneider<sup>3)</sup>, Laura Marín-Samper<sup>4)</sup>, Javier Arístegui<sup>4)</sup>, Phil Renforth<sup>5)</sup>, Jan Taucher<sup>3)</sup>, Ulf Riebesell<sup>3)</sup>

1) Institute for Geology, Universität Hamburg, Bundesstrasse 55, D-20146 Hamburg, Germany

2) Faculty of Physics/Electrical Engineering, Universität Bremen, Otto-Hahn-Allee 1, 28359 Bremen, Germany

3) Geomar Helmholtz Centre for Ocean Research Kiel, Kiel, Germany

4) Instituto de Oceanografía y Cambio Global, Universidad de Las Palmas de Gran Canaria, Las Palmas, Spain

5) School of Engineering and Physical Sciences, Heriot-Watt University, Edinburgh, EH14 4AS, UK

\*) These authors contributed equally

Correspondence to: Jens Hartmann ([geo@hattes.de](mailto:geo@hattes.de)), Niels Suitner ([niels.suitner@uni-hamburg.de](mailto:niels.suitner@uni-hamburg.de))

**Abstract.** According to modelling studies, ocean alkalinity enhancement (OAE) is one of the proposed carbon dioxide removal (CDR) approaches with large potential, and the beneficial side effect of counteracting ocean acidification. The real-world application of OAE, however, remains unclear as most basic assumptions are untested. Before large-scale deployment can be considered, safe and sustainable procedures for the addition of alkalinity to seawater must be identified and governance established. One of the concerns is the stability of alkalinity when added to seawater. The surface ocean is already supersaturated with respect to calcite and aragonite, and an increase in total alkalinity (TA) together with a corresponding shift in carbonate chemistry towards higher carbonate ion concentrations would result in further increase in supersaturation, and potentially to solid carbonate precipitation. Precipitation of carbonate minerals consumes alkalinity and increases dissolved CO<sub>2</sub> in seawater, thereby reducing the efficiency of OAE for CO<sub>2</sub> removal. In order to address the application of alkaline solution as well as fine particulate alkaline solids, a set of six experiments was performed using natural seawater with alkalinity of around 2400 µmol/kgsw. The application of CO<sub>2</sub>-equilibrated alkaline solution bears the lowest risk of losing alkalinity due to carbonate phase formation if added total alkalinity ( $\Delta$ TA) is less than 2400 µmol/kgsw. The addition of reactive alkaline solids can cause a net loss of alkalinity if added  $\Delta$ TA > 600 µmol/kgsw (e.g., for Mg(OH)<sub>2</sub>). Commercially available (ultrafine) Ca(OH)<sub>2</sub> causes, in general, a net loss in TA for the tested amounts of TA addition, which has consequences for suggested use of slurries with alkaline solids supplied from ships. The rapid application of excessive amounts of Ca(OH)<sub>2</sub>, exceeding a threshold for alkalinity loss, resulted in a massive increase in TA (> 20,000 µmol/kgsw) at the cost of lower efficiency and resultant high pH values > 9.5. Analysis of precipitates indicates formation of aragonite. However, unstable carbonate phases formed can partially redissolve, indicating that net-loss of a fraction of alkalinity may not be permanent, which has important implications for real world OAE application.

Our results indicate that using an alkaline solution instead of reactive alkaline particles can avoid carbonate formation, unless  
35 alkalinity addition via solutions shifts the system beyond critical supersaturation levels. To avoid the loss of alkalinity and  
dissolved inorganic carbon (DIC) from seawater, the application of reactor techniques can be considered. These techniques  
produce an equilibrated solution from alkaline solids and CO<sub>2</sub> prior to application. Differing behaviours of tested materials  
suggest that standardized engineered materials for OAE need to be developed to achieve safe and sustainable OAE with solids,  
if reactors technologies should be avoided.

## 40 **1 Introduction**

The impacts of climate warming are increasingly severe (IPCC, 2021). To tackle this problem, the 2°C target was stipulated  
in the 2015 Paris Agreement (UNFCCC, 2015). While many countries claim to have shown efforts to decrease greenhouse gas  
emissions since, the overall emissions are still rising (Friedlingstein et al., 2021) and it seems now improbable to reach the  
target by mitigation alone, without the help of negative emission technologies (NETs) (IPCC, 2021). However, most discussed  
45 NETs or carbon dioxide removal (CDR) technologies are still immature for upscaling or even ready for operation.

Ocean Alkalinity Enhancement (OAE) is one of the CDR strategies being considered (NASSEM, 2022). However, its potential  
impacts are not well understood as well as practicalities of operating at scale, like suitable approaches to monitoring and  
verification. This is due to the lack of laboratory and field experiments targeting OAE, while laboratory experiments, focusing  
on seawater carbonate chemistry in general, exist in large quantity, with limited implication for OAE application.  
50 Consequences of application and techniques for optimal deployment need therefore to be determined to develop sustainable  
ways of OAE. A number of model studies exist (Fakhraee et al., 2022; González and Ilyina, 2016; Ilyina et al., 2013; Kheshgi,  
1995; Lenton et al., 2018) focusing on the consequences of OAE at the global scale or the applicability via (cargo) ships  
(Caserini et al., 2021). They are, however, based on a series of assumptions, e.g., that added alkalinity remains stable, is not  
lost, or negative net change in TA due application of OAE is not a consequence, and that alkalinity can be technically added  
55 to seawater.

One of the key questions to be solved for OAE is the stability of the added alkalinity (Moras et al., 2021). Additional alkalinity  
loss via carbonate phase formation (causing CO<sub>2</sub> leakage), either via inorganic processes or triggered by biological activity,  
should be avoided. The carbonate supersaturation level is a driver for possible formation of new carbonate phases (Koishi,  
2017). Nucleation of new phases is the greatest energy barrier to encompass before crystal growth can continue (Sun et al.,  
60 2015). After nucleation from a bulk solution and for the growth to proceed, a further energy barrier at the interface between  
the new phase and the surrounding solution matrix must be overcome (Koishi, 2017; Sear, 2007).

Carbonate nucleation in seawater, filtered with 0.2 µm filters to remove particles, with a salinity around 35 at 25°C, starts at a  
saturation level of  $\Omega_{\text{calcite}}$  around 19-20 (Morse and He, 1993), which corresponds to an  $\Omega_{\text{aragonite}}$  of around 12.5-13.5, depending  
on temperature and salinity. The filtering of water is for avoiding nuclei for condensation or providing surfaces for carbonate  
65 formation (Wurgaft et al., 2021). The energy barrier for carbonate formation on suitable surfaces, like on existing carbonate is

however lower. One of the until now unclear aspects in context of OAE is at which saturation levels carbonate formation in seawater occurs after application of alkalinity and at which time after application this is triggered. In addition, the abundance of possible seed particles and their surface area provided (quality and quantity) for possible heterogenous carbonate formation triggering an alkalinity loss needs to be understood for OAE management.

- 70 Addition of alkalinity without equilibrating the water with the atmospheric CO<sub>2</sub> causes high saturation levels (due to more pronounced shifts in the carbonate system). Even under optimal natural conditions for air-sea gas exchange, CO<sub>2</sub> equilibration could take weeks to months (Jones et al., 2014). Such a non-equilibrated system would be representative for any OAE application where CO<sub>2</sub> uptake is not actively facilitated, or where ocean mixing of waters and ingassing is slow. Alternatively, OAE procedures could be conducted in a way that saturation levels after alkalinity application remain low, for example by
- 75 equilibrating the ocean water with CO<sub>2</sub> artificially or using substances which allow for lower saturation levels. Part of the applied alkalinity due OAE procedures maybe lost due carbonate formation, meaning that OAE efficiency should be rated based on the net alkalinity added:

$$\Delta TA_{\text{net}} = TA_{\text{final}} - TA_{\text{initial}} = \Delta TA_{\text{added}} + \Delta TA_{\text{loss}}$$

$\Delta TA_{\text{net}}$ : net change of TA

$TA_{\text{final}}$ : absolute reached TA after TA addition (measured)

$TA_{\text{initial}}$ : initial TA of used seawater (measured)

$\Delta TA_{\text{added}}$ : amount of increased TA by alkalinity addition

$\Delta TA_{\text{loss}}$ : amount of TA decline during the experiment (negative sign)

In order to test for the stability of alkalinity after simulated OAE application, this study aims to address the following five questions using insights from six conducted experiments:

- 80
- 1) What is the efficiency advantage using preproduced, CO<sub>2</sub>-equilibrated alkaline solutions over non-equilibrated alkaline solutions?
  - 2) Do naturally occurring particles or added particles in the ocean water affect the stability range of added alkalinity?
  - 3) Are fast reacting solid alkaline materials like Ca(OH)<sub>2</sub> or even slower ones like Mg(OH)<sub>2</sub> useful for adding alkalinity
  - 85 to the seawater?
  - 4) Does lost alkalinity due to carbonate formation recover due to redissolution to some part?
  - 5) At which elevated bulk solution saturation levels can potential loss of alkalinity be expected after how much time?

## 2 Methods

In order to understand the consequences of different application procedures, materials and boundary conditions for sustainable application of OAE, a set of six experiments was designed (Table 1) using these basic system setups:

- I A CO<sub>2</sub>-equilibrated system, using an aqueous solution for OAE, testing 4 days.  
 II A non-CO<sub>2</sub>-equilibrated system using an aqueous solution for OAE, testing 4 days.  
 III A CO<sub>2</sub>-equilibrated system with/without added carbonate particles and, using aqueous solution for OAE, testing a period of ~90 days.  
 IV A non CO<sub>2</sub>-equilibrated system, using solid particles of magnesium hydroxide (Mg(OH)<sub>2</sub>) for OAE, testing 4 days.  
 V A non CO<sub>2</sub>-equilibrated system, using solid alkalinity of Ca(OH)<sub>2</sub> for OAE and forcing TA loss to study TA recovery potential, testing 10 days.  
 VI Adding excessive amounts of alkaline particles to test if TA-loss can be avoided, testing 24 hours.

#	abiotic biotic	material	CO <sub>2</sub>	water	setup			ΔTA <sub>added</sub> [μmol/kgw]	concept [related research questions]
					filter	reactor	storage		
I	a	Na <sub>2</sub> CO <sub>3</sub> / NaHCO <sub>3</sub>	eq.	GC	0.2 μm	0.5 L bottle	dark	0-2,400	CO <sub>2</sub> -equilibrated, ΔTA <sub>added</sub> steps of 300 μmol/kgw, TA-addition with stock solution, runtime 4 days [1]
	b				55 μm	1.2 L bottle	climate chamber	0-1,200	
II	a	NaOH	neq.	GC	0.2 μm	0.5 L bottle	dark	0-2,400	Non-CO <sub>2</sub> -equilibrated, ΔTA <sub>added</sub> steps of 300 μmol/kgw, TA-addition with stock solution, runtime 4 days [1, 2, 5]
	b				55 μm	1.2 L bottle	climate chamber	0-1,200	
III	b	Carbonate precipitate	eq.	GC	-	8 L bottle	harbour	0/2,100/ 2,400	CO <sub>2</sub> -equilibrated, TA-addition with stock solution, trigger precipitation with seed material, 90 days [2, 5]
IV	a	Mg(OH) <sub>2</sub>	neq.	GC	0.2 μm	1.2 L bottle	climate chamber	0-2,400	Non-CO <sub>2</sub> -equilibrated, ΔTA <sub>added</sub> steps of 600 μmol/kgw, TA-addition with solid alkaline material, runtime 4 days [2, 3, 5]
	b				55 μm			+34,288	
V	a	Ca(OH) <sub>2</sub>	neq.	N.-Sea	0.2 μm	0.5 L flask	shaking table	5,400	pH/TA development over 10 days, redissolution, solid alkaline material [3, 4]
VI	a	Mg(OH) <sub>2</sub> / Ca(OH) <sub>2</sub>	neq.	N.-Sea	0.2 μm	0.5 L flask	shaking table	-	TA loss/gain of various weights of added solid alkaline materials, runtime 1 day [3]

**Table 1:** Overview of the 6 experiments conducted (I-VI). Abbreviations: abiotic (a), seawater filtered with 0.2 μm filters to remove plankton, and biotic (b), seawater filtered with 55 μm filters to remove larger plankton. The column CO<sub>2</sub> refers to equilibrated to atmospheric CO<sub>2</sub> levels (eq.) or not (neq.), water: origin of used seawater (GC – Gran Canaria/Taliarte and North Sea, see below for details). ΔTA<sub>added</sub> is the range of added alkalinity per experiment. Numbers of the related research questions (see Introduction) are given in the concept column in brackets.

To examine how planktonic organisms and particles naturally occurring in the ocean might affect OAE performance, e.g., by serving as condensation nuclei for mineral precipitation, we performed two separate sets of experiments including and  
110 excluding biogenic particles (termed biotic and abiotic hereafter). For the abiotic approach seawater was filtered through a 0.2  $\mu\text{m}$  PC-filter. Seawater for the 'biotic' approach was filtered through a 55  $\mu\text{m}$  filter to exclude larger and rare organisms (e.g., mesozooplankton), but keep the remainder.

For all experiments **I** to **IV**, oligotrophic coastal seawater ( $\text{TA}_{\text{initial}} \approx 2411 \mu\text{mol/kgsw}$ ,  $\text{S} \approx 36.6$ ,  $\text{pH} \approx 8.15$ ,  $\text{T} \approx 23^\circ\text{C}$ ) was taken at 4 meters depth in the vicinity of the harbour of Taliarte, Gran Canaria, on 2021-09-16 (**I+II+IV**) and 2021-09-30 (**III**).  
115 Seawater for the alkalinity recovery test, experiment **V**, was taken from the open North Sea (German Bight, N 54.93 E 6.43,  $\text{TA}_{\text{initial}} \approx 2297 \mu\text{mol/kgsw}$ ,  $\text{S} \approx 32.9$ ,  $\text{pH} \approx 8.18$ ,  $\text{DSi} 16 \mu\text{mol/L}$ ). CO2SYS (Pierrot et al., 2006) was used to determine the amount of alkaline solution/solid material needed to increase TA in several steps.

## 2.1 Experiment I and II: Comparing CO<sub>2</sub> equilibrated versus non-equilibrated alkalinity enhancement

For the abiotic **equilibrated system (Ia)** nine batch solutions were prepared adding TA in nine steps of 300  $\mu\text{mol/kgsw}$ ,  
120 starting at an initial alkalinity value of  $\sim 2400 \mu\text{mol/kgsw}$  (fresh untreated seawater,  $\Delta\text{TA}_0$ ), with a maximum final treatment of  $\text{TA}_{\text{final}} \sim 4800 \mu\text{mol/kgsw}$  ( $\Delta\text{TA}_{2400}$ ). The TA-enhancement was achieved by adding calculated volumes of 0.5 M  $\text{NaHCO}_3$  and 0.5 M  $\text{Na}_2\text{CO}_3$  solutions using calculations from CO2SYS to ensure CO<sub>2</sub>-equilibrated conditions (420 ppm – see attached data table for added volumes). While preparing stock solutions with  $\text{NaHCO}_3/\text{Na}_2\text{CO}_3$ , solids dissolved entirely within seconds to several minutes. After taking an initial sample (day 0) from every batch, the remaining solutions were filled in portions of  
125 400.0 g  $\pm$  0.5 g into 500 ml Dickson bottles (bottles for seawater TA and DIC standards), each for a duration of 24 h or 96 h. All bottles were stored in the dark, unsealed – open to the laboratory atmosphere and kept at a constant temperature of 24  $^\circ\text{C}$ . The exact same procedure was followed for the abiotic **non-equilibrated system (IIa)**, except using a 0.5 M NaOH solution for the alkalinity enhancement and preventing gas exchange by filling the bottle to the top ( $\approx 525$  g) and capping them airtight without headspace.

130 For the biotic **equilibrated system (Ib)** and **non-equilibrated system (IIb)** 1.2-L polycarbonate bottles were used, both filled to the top and capped airtight. Bottles were stored in a climate chamber (24  $^\circ\text{C}$  and 12/12 hours light/dark intervals) over the duration of the experiment to ensure a stable environment for the microbial community. The same seawater, resources and procedures for alkalinity enhancement were utilized as in the abiotic experiments **Ia** and **IIa**. Samples were taken just at the start (day 0) and the end of the experiment (day 4) to avoid headspace in the bottles. Starting with the initial value of seawater  
135 ( $\text{TA}_{\text{initial}}/\Delta\text{TA}_0$ ) the alkalinity was increased in eight 150  $\mu\text{mol/kgsw}$  steps to 3600  $\mu\text{mol/kgsw}$  ( $\Delta\text{TA}_{1200}$ ).

## 2.2 Experiments III: Testing the role of particles as condensation nuclei for mineral precipitation

We prepared a solution in equilibrium with the atmosphere as described for experiment **I** for the two highest  $\Delta\text{TA}$  treatments, namely  $\Delta\text{TA}_{2100}$ ,  $\Delta\text{TA}_{2400}$ . Solutions were placed into 8L PET bottles in two treatments: one without adding particles and one with adding previously precipitated carbonates (120 mg wet weight each) as seed material (precipitation nuclei), retrieved

140 from a preceding experiment. The closed bottles were placed next to the pier in the harbour of Taliarte, Gran Canaria, about 1.5 m below the water surface with average water temperatures around 20-23°C. Samples of 150 ml each were taken at days 0, 2, 4, 6, 8 and 10. After the 10 days of experiment the content of the bottles was transferred to 500 ml Dickson bottles and left alone closed to the atmosphere and in the dark for another 80 days. Two additional samples (40 ml each) were collected at days 46 and 90.

## 145 **2.3 Experiments IV, V and VI: Testing alkalisation with solid Mg(OH)<sub>2</sub> and Ca(OH)<sub>2</sub>.**

### **2.3.1 Experiment IV: Mg(OH)<sub>2</sub>**

While for experiments **I** and **II** fast dissolving materials with relatively high solubilities were used to produce an alkaline solution, solid materials were used in experiments **IV, V & VI**. Magnesium hydroxide in experiment **IV** was added as a powder directly into the reactor bottles. Because of a lower reactivity the material was not to be expected to dissolve immediately, so  
150 dissolution took place throughout the experimental duration of four days. Two different Mg(OH)<sub>2</sub> materials from the companies (Negative Emissions Materials (brucite I) and Carl Roth (brucite II)) were utilized to compare their behaviour in dissolution and generation of alkalinity. Brucite I is a substance derived from the dissolution of olivine rich material, brucite II an industrial product prepared for rapid dissolution. Both, abiotic and biotic approaches (distinction 0.2 µm filtration) were conducted in 1.2-L PC bottles and followed the same procedure as in **Ib** and **Iib**, filled airtight to the top and kept in the climate  
155 chamber, after mixing them gently for 5 minutes. The mass of added magnesium hydroxide was calculated to yield the same increase in alkalinity as in experiments **I** and **II**, assuming total dissolution could be achieved. The target concentrations ranged from 12.8 mg/kgsw to 666 mg/kgsw and representing solid alkalinity addition of 600, 1200, 1800, 2100, 2400 and 34288 µmol/kgsw in ΔTA<sub>added</sub>. The latter high addition was intended to simulate an approach assuming large amounts of particles being added, e.g., via ship disposal. The mixing at the beginning should simulate turbulence during application,  
160 assuming further low to no turbulence. Given the further still water a scenario is simulated, which lowers the particle boundary layer dynamics. This can be seen as a baseline scenario, where more turbulence might cause higher dissolution rates. In experiment **IV** liquid subsamples were taken at the start of the experiment and after 24 and 96 hours. The brucite material was dried at 40°C for 72 hours before the experiments.

### **2.3.2 Experiment V: Alkalinity recovery after mineral precipitation**

165 This experiment focused on the addition of alkalinity due to redissolution of instable alkaline phases formed after Ca(OH)<sub>2</sub> application causing an initial net loss of TA. 0.2 g Ca(OH)<sub>2</sub> (ΔTA<sub>added</sub> ≈ 5400 µmol/kgsw) were dissolved in 500 ml PC-Erlenmeyer-flasks filled with 300 g of North Sea water (0.2 µm filtered) and left open to the laboratory atmosphere at 23 °C. The experiment was conducted in 12 timesteps lasting from 15 min to 10 days, for each timestep with three replicates and one control flask each without any added material. All experimental flasks were permanently placed on a shaking table (120 rpm,

170 the maximum frequency without risking loss of water and to simulate favourable conditions for gas exchange). The pH of the seawater was continuously monitored in 5 minutes steps. About 100 ml per sample were used for the measurements.

### 2.3.3. Experiment VI: Thresholds – the swing from TA loss to TA gain again

The experiment was set up to check if potential threshold values for net TA loss/gain with the combined effects of alkaline material addition plus mineral precipitation after 24 hours exist in case larger amounts of solids are dissolved than in the  
175 previous experiments, resulting in the net loss of TA. A gradient of added solid masses to seawater, using the brucite II (experiment IV) and the Ca(OH)<sub>2</sub> (experiment V) were used. For this the same seawater as in experiment V was used adding up to 13.3 g brucite or 2 g Ca(OH)<sub>2</sub> per kg of seawater and measuring TA after 24 hours (see attached data tables for details). The same bottles (500 ml PC flasks) and experimental setup (shaking table) than in experiment V was used.

### 2.3 Measurements

180 Immediately after the end of an experiment each sample was filtered (0.2 µm – using Nalgene filtration bottles) to stop possible further reaction on larger particles and remove the biomass from the biotic approaches for further analysis. While filtering, all systems were kept airtight as much as possible to prevent gas exchange with the atmosphere. Samples which were analyzed for DIC were filtered with a peristaltic pump and an attached 0.2 µm syringe filter to minimize the air exchange. Samples were measured for total alkalinity (TA), pH, salinity, conductivity, temperature, and biotic samples from experiment I and II for  
185 dissolved inorganic carbon (DIC). TA was determined by titration with 0.1 M hydrochloric acid within an 862 Compact Titrosampler (Metrohm) – for samples of day 46 and 90 in experiment III and all samples of experiment V a different titrator (888 Titrande, Metrohm) with a 0.02 M hydrochloric acid was used. DIC was analysed by infrared absorption, using a LI-COR LI-7000 on an AIRICA system (MARIANDA, Kiel). Calibration of TA and DIC measurements was determined against certified reference materials (CRM batches 143 and 190), supplied by A. Dickson, Scripps Institution of Oceanography (USA).  
190 Single determinations were made for TA measurement, except for experiments Ia and IIa, which were made on two technical replicates. DIC was measured on 2-3 technical replicates. Final values are numerical averages of these replicates. To analyse for pH, salinity, conductivity and temperature a WTW multimeter (MultiLine® Multi 3630 IDS, pH-probe: SenTix 940 pH-electrode, conductivity: TetraCon 925 cell, Xylem) was employed. The pH-probe was calibrated with WTW buffer solutions according to NIST/PTB in 4 steps (1.679-9.180 at 25°C), and corrected for seawater after Badocco et al. (2021). For the  
195 TetraCon 925 cell 0.01 mol/L KCl calibration standards for conductivity cells (WTW, traceable to NIST/PTB) was used. Variables such as DIC, pCO<sub>2</sub> or aragonite saturation state ( $\Omega_{\text{aragonite}}$ ) were calculated using measured values of TA and pH (or DIC in case of experiment Ib and experiment IIb) with CO2SYS version 2.5 Excel sheet (Pierrot et al., 2006), including error propagations based on Orr et al. (2018). The constants in CO2SYS were set to: Lueker et al. (2000) for K1 and K2; Dickson (1990) for KHSO<sub>4</sub>; Dickson and Riley (1979) for KHF and Uppström (1974) for [B]<sub>T</sub>Value, while using the seawater pH  
200 scale, were used. Filtrates of experiment IIa (day 0, 1 and 4) and V (day 10) were analyzed by scanning electron microscopy

(SEM) using a Tabletop Microscope Hitachi TM4000plus equipped with an Energy-dispersive X-ray spectroscopy (EDX – Bruker Q75), to provide data for the elemental composition and a visual impression of precipitates.



### 3 Results

#### 3.1 Experiment I: Equilibrated alkalisation

205 By adding defined amounts of a  $\text{NaHCO}_3/\text{Na}_2\text{CO}_3$  solution,  $\text{CO}_2$ -equilibrated  $\Delta\text{TA}_{\text{added}}$  steps of 300  $\mu\text{mol/kgsw}$  for abiotic and 150  $\mu\text{mol/kgsw}$  for biotic approaches was achieved, yielding a range from  $\Delta\text{TA}_0$  ( $\text{TA}_{\text{final}} = 2411 \mu\text{mol/kgsw}$ ,  $\Omega_{\text{aragonite}} = 4.2$ ,  $\text{pH} = 8.15$ ) up to  $\Delta\text{TA}_{2400}$  ( $\text{TA}_{\text{final}} = 4750 \mu\text{mol/kgsw}$ ,  $\Omega_{\text{aragonite}} = 13.2$ ,  $\text{pH} = 8.45$ ) for the abiotic and  $\Delta\text{TA}_{1200}$  ( $\text{TA}_{\text{final}} = 3567 \mu\text{mol/kgsw}$ ,  $\Omega_{\text{aragonite}} = 6.4$ ,  $\text{pH} = 8.15$ ) for the biotic experiment (Fig. 1). Achieved additions vary slightly from the targeted additions. The seawater TA was monitored after the initial alkalinity addition to determine if any alkalinity was lost

210 subsequently due to carbonate phase formation processes. The alkalinity enhancement has taken place almost in a linear manner close to ideal ('1:1' dotted-grey line in Fig. 1a and d). As the solution was initially  $\text{CO}_2$ -equilibrated with current atmospheric conditions, DIC,  $\Omega_{\text{aragonite}}$  and pH-value increased proportionally. No detectable loss in TA was observed after 1 and 4 days following the initial TA addition at time 0 for either the abiotic (0.2  $\mu\text{m}$  filtered) or in the biotic (55  $\mu\text{m}$  filtered) treatment, including living planktonic organisms.  $\Omega_{\text{aragonite}}$  values remained with exception of its highest value of 13.2 below

215 the critical threshold of around 12.5 for  $\Omega_{\text{aragonite}}$  at salinity of 36.5 (corresponding to  $\Omega_{\text{calcite}} \sim 19$  as identified by Morse and He (1993)), and prevented a potential loss of alkalinity due to precipitation. The pH-value followed a quasi-linear trend with  $\Delta\text{TA}_{\text{added}}$ , and increased to 8.45 for the abiotic  $\Delta\text{TA}_{2400}$  treatment (Fig. 1c). A relatively small decline in pH and  $\Omega_{\text{aragonite}}$  in the abiotic, equilibrated experiment can be observed.

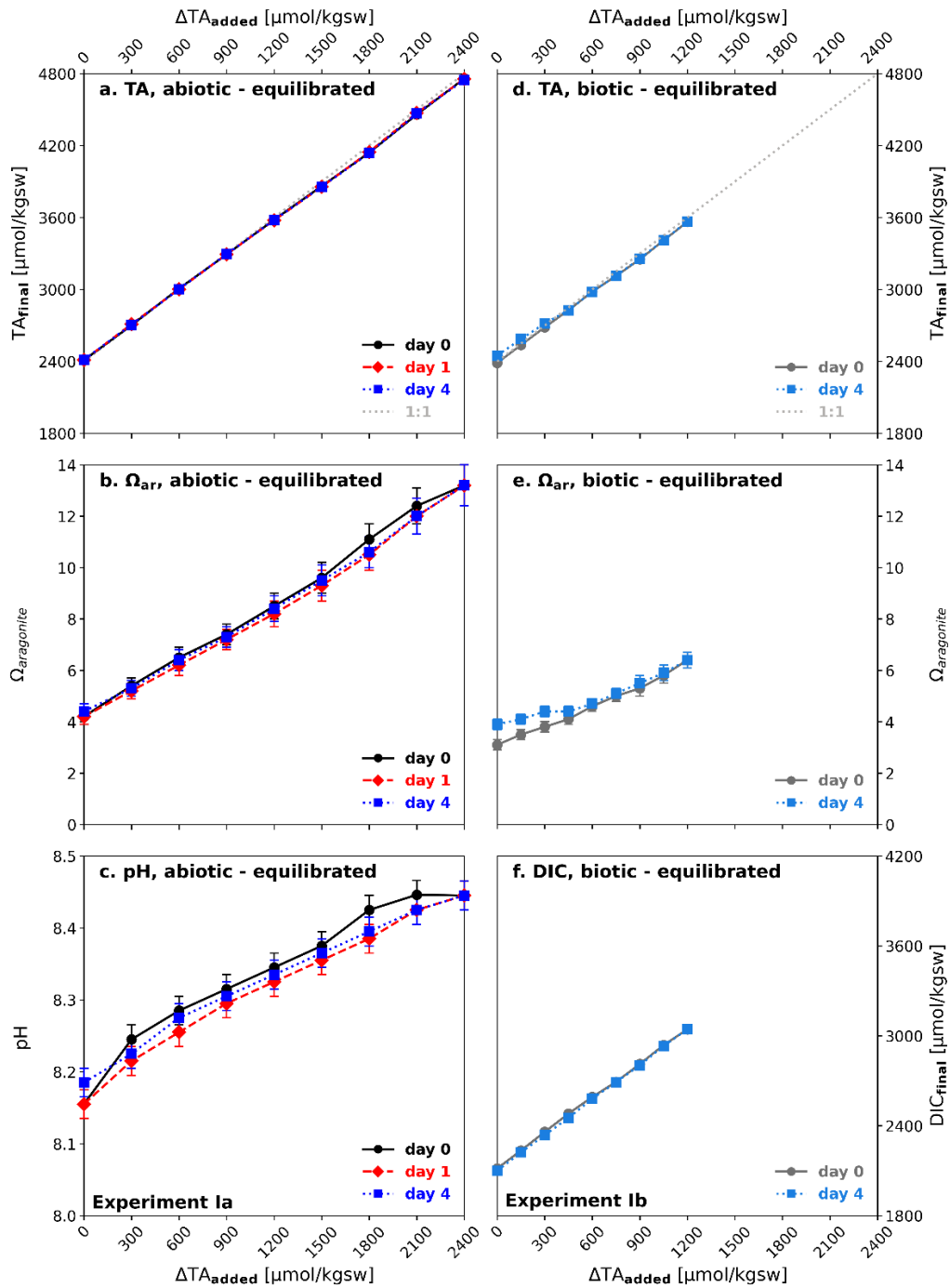
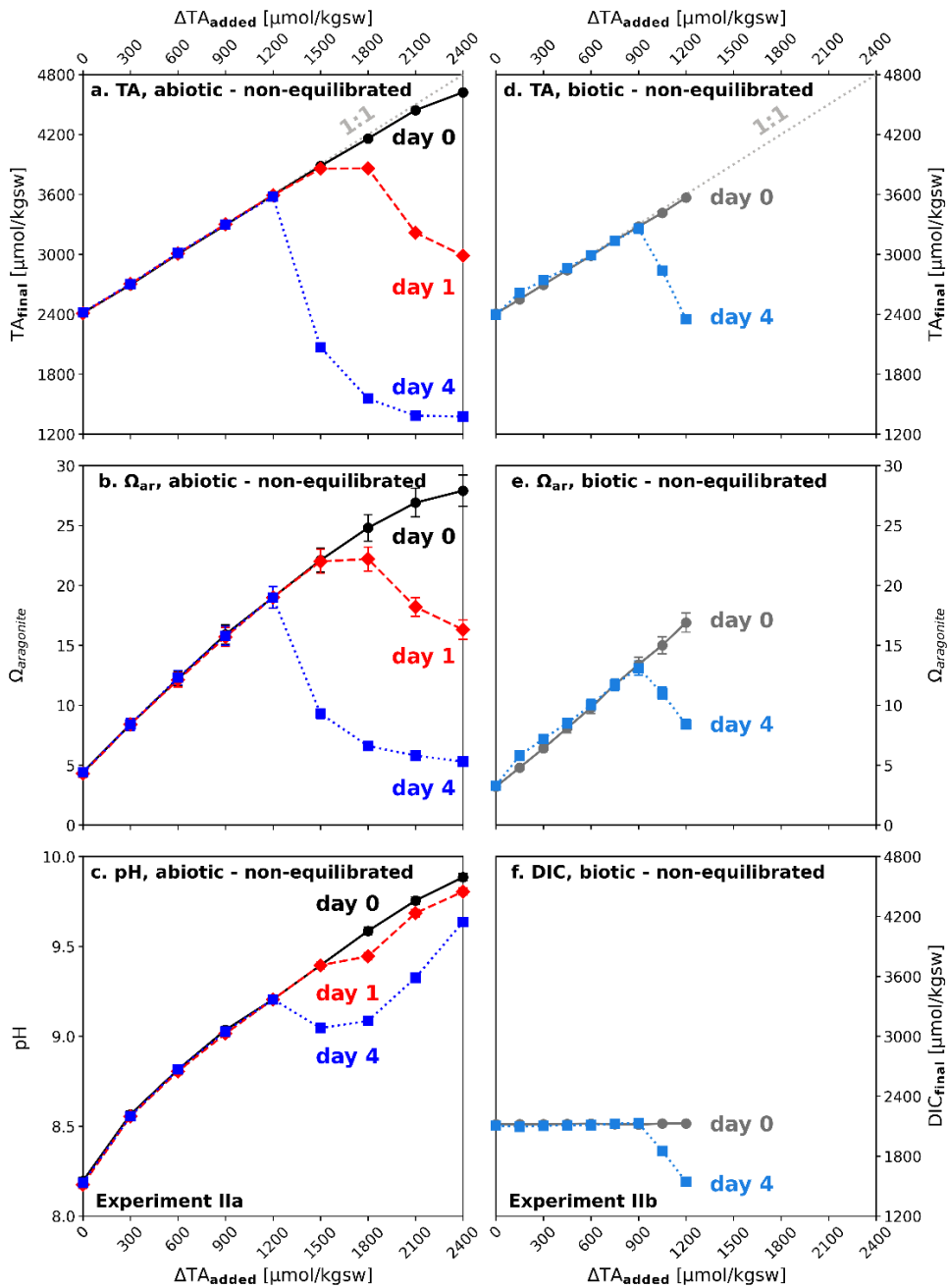


**Figure 1: Temporal development after CO<sub>2</sub> equilibrated alkalisation:** (a, b, c) experiment Ia, (d, e, f) experiment Ib; (a, d)  $\Delta TA_{\text{added}}$  vs.  $TA_{\text{final}}$ ; (b, e) aragonite saturation state ( $\Omega_{\text{aragonite}}$ ) in relation to  $\Delta TA_{\text{added}}$ ; (c) pH in relation to  $\Delta TA_{\text{added}}$ ; (f)  $DIC_{\text{final}}$  in relation to  $\Delta TA_{\text{added}}$ . Black/grey symbols correspond to start of the experiment, red after 1 day and blue after 4 days.  $TA_{\text{initial}}$  conditions of used seawater:  $\Delta TA_0 \approx 2411 \mu\text{mol/kgsw}$ ,  $\Omega_{\text{Ar}} = 4.2$ , pH = 8.15.

### 3.2 Experiment II: Non-equilibrated alkalinisation

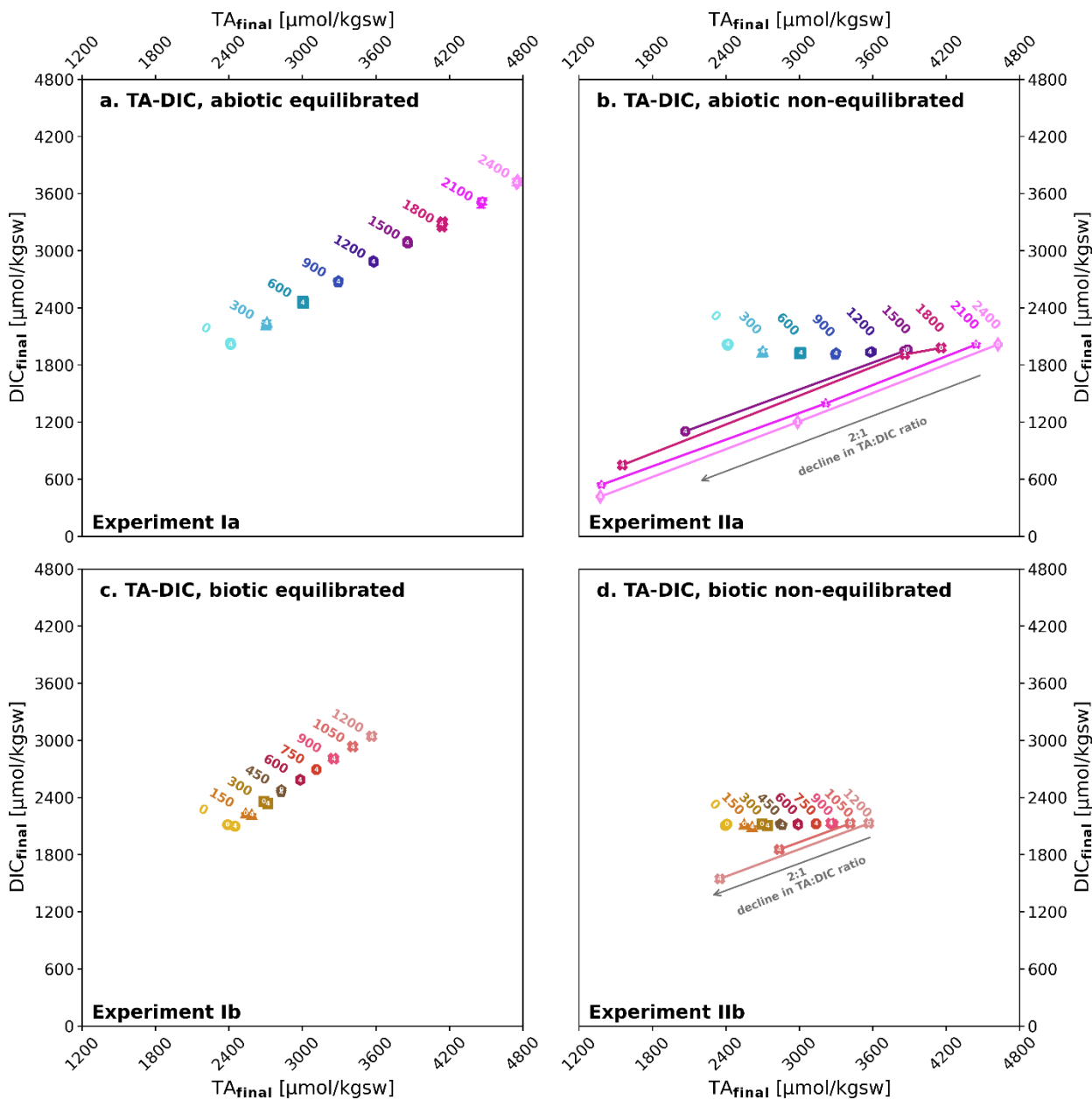
225 In the non-equilibrated experiments II, solely TA was increased by using a 0.5 M NaOH stock solution while DIC remained  
at the initial seawater level of 2006  $\mu\text{mol/kgsw}$ . Equilibration with the atmosphere was inhibited by closing the sample  
containers airtight.  $\text{TA}_{\text{initial}}$  increased at the highest level ( $\Delta\text{TA}_{2400}$  with target level of  $\sim 4800$   $\mu\text{mol/kgsw}$ ) to only 4622  
 $\mu\text{mol/kgsw}$  ( $\text{TA}_{\text{final}}$ ) in the abiotic approach, with  $\Omega_{\text{aragonite}} \sim 28$  and a pH of 9.89. An immediate precipitation of 0.1-2 cm long  
mineral needles was observed floating in the abiotic reactor bottles just seconds after TA addition, suggesting nucleation  
230 happens in the water. Precipitation on the wall of the vessel was not visible by eye. This is also reflected by a slight deviation  
from the idealised TA-addition line in Fig. 2a ('1:1' dotted-grey line), which indicates a noticeable decrease for the two highest  
TA additions ( $\Delta\text{TA}_{2100}$  and  $\Delta\text{TA}_{2400}$ ).  $\Delta\text{TA}_0$  to  $\Delta\text{TA}_{1800}$  maintained their intended alkalinity in both the abiotic and biotic  
treatments on day 0. After 1 day alkalinity loss can also be observed for  $\Delta\text{TA}_{1800}$ . The decline in TA for the three highest TA  
additions was now accompanied by visible precipitation on the inner wall of the reactors, suggesting that at this stage wall  
235 surfaces of the vessel acted as nucleation points. Alkalinity loss continued and on day 4 was also detected in the next lower  
treatment. At this stage the alkalinity in the four highest treatments dropped below values prior to alkalinity addition, marking  
a net loss of alkalinity compared to the initial seawater water level. Associated to this,  $\Omega_{\text{aragonite}}$  declined to values of 5.3 to 6.6  
on day 4 (Fig. 2b), approaching the initial value of  $\sim 4.2$ . pH, on the other hand, remained comparatively high, with only small  
decreases of 0.3-0.5 units down to values of 9.1-9.6 (Fig 2). In the abiotic treatments  $\Delta\text{TA}_0$  to  $\Delta\text{TA}_{1200}$  alkalinity was stable  
240 and no precipitation was observed within the first four days, despite that for treatments  $\Delta\text{TA}_{900}$  &  $\Delta\text{TA}_{1200}$   $\Omega_{\text{aragonite}}$  was above  
the critical value. In contrast, in the biotic setup alkalinity loss occurred in  $\Delta\text{TA}_{1050}$  and  $\Delta\text{TA}_{1200}$  treatments at least on day 4,  
i.e. at lower alkalinity additions than in the abiotic treatments (Fig. 2d), with corresponding declines in  $\Omega_{\text{aragonite}}$  and DIC (Fig.  
2e and f).



245 **Figure 2: Temporal development after non-equilibrated alkalinisation:** (a, b, c) experiment IIa, (d, e, f) experiment IIb; (a, d)  $\Delta\text{TA}_{\text{added}}$  vs.  $\text{TA}_{\text{final}}$ ; (b, e) aragonite saturation state ( $\Omega_{\text{aragonite}}$ ) in relation to  $\Delta\text{TA}_{\text{added}}$ ; (c) pH in relation to  $\Delta\text{TA}_{\text{added}}$ ; (f)  $\text{DIC}_{\text{final}}$  in relation to  $\Delta\text{TA}_{\text{added}}$ . Black/grey symbols correspond to start of the experiment, red after 1 day and blue after 4 days. Note the different ranges of  $\Delta\text{TA}_{\text{added}}$  in the abiotic and biotic set-up. The slightly higher start  $\Omega_{\text{aragonite}}$  for the biotic treatment at day 4 compared to day 1 is because  $\Omega_{\text{aragonite}}$  was calculated by TA and DIC, while for the abiotic experiment using TA and pH.

### 250 3.3 Experiments I & II: TA/DIC development in equilibrated versus non-equilibrated alkalisation

While in the experiment simulating equilibrated alkalisation TA and DIC were added (as  $\text{NaHCO}_3$  and  $\text{Na}_2\text{CO}_3$ ) in proportions (Fig. 3a, c) to maintain close to atmospheric  $\text{CO}_2$  levels, in the non-equilibrated alkalisation experiment only TA was added (as  $\text{NaOH}$ ) (Fig. 3b, d), simulating alkalisation without any  $\text{CO}_2$  equilibration. Whereas the former yielded comparatively moderate changes in seawater carbonate chemistry, with only one  $\Omega_{\text{aragonite}}$  value slightly above the critical threshold of around 12.5 (identified by Morse and He, 1993), the non-equilibrated approach caused strong changes in the carbonate system with  $\Omega_{\text{aragonite}}$  values above 20 for  $\Delta\text{TA}_{1500}$  to  $\Delta\text{TA}_{2400}$  and between 15 and 17 for  $\Delta\text{TA}_{1050}$  to  $\Delta\text{TA}_{1200}$ , i.e. well above the critical threshold. Consequently, while precipitation was absent in the abiotic and biotic set-up in the equilibrated treatment, strong alkalinity loss through precipitation occurred in the non-equilibrated experiment. While in the biotic set-up precipitation was observed at  $\Delta\text{TA}_{1050}$  and  $\Delta\text{TA}_{1200}$  (starting  $\Omega_{\text{aragonite}}$  15 and 17, Fig. 2b), in the abiotic set-up precipitation only occurred at and above  $\Delta\text{TA}_{1500}$ , with no detectable precipitation at  $\Delta\text{TA}_{900}$  and  $\Delta\text{TA}_{1200}$  (starting  $\Omega_{\text{aragonite}}$  16 and 19, Fig. 2e). The loss-ratio in TA:DIC was about 2:1 (Fig. 3b, d) in all treatments, indicating the loss of alkalinity due to the precipitation of carbonates. Loss-ratio in TA:DIC for the abiotic set-up were 2.12 for  $\Delta\text{TA}_{1500}$ , 1.98 for  $\Delta\text{TA}_{1800}$ , 2.06 for  $\Delta\text{TA}_{2100}$ , and 2.03 for  $\Delta\text{TA}_{2400}$  and for the biotic set-up 2.11 for  $\Delta\text{TA}_{1050}$  and 2.09 for  $\Delta\text{TA}_{1200}$ .

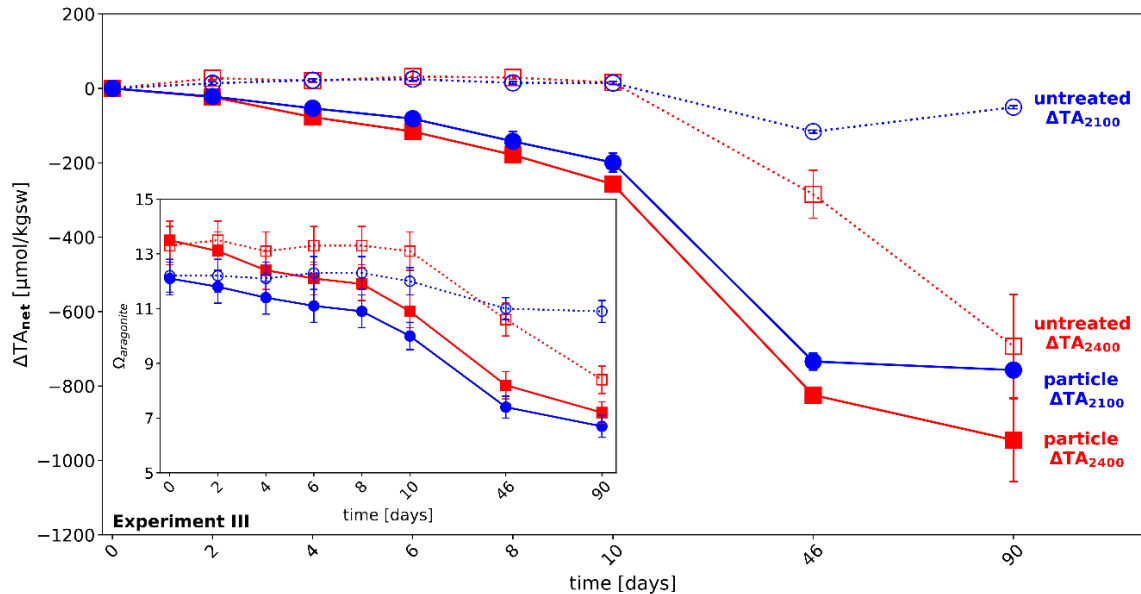


265 **Figure 3: TA<sub>final</sub> versus DIC<sub>final</sub> at the start of the experiments I and II and after precipitation;** (a-b) abiotic after 0, 1 and 4 days, (c-d) biotic after 0 and 4 days, equilibrated alkalisation (left, experiment I), non-equilibrated alkalisation (right, experiment II). The TA:DIC change ratio of 2:1 indicates that alkalinity loss was due to carbonate precipitation. Sampling days (0, 1 and 4) are written on top of each datapoint marker. Due to overlapping in case of no change in data, the marker description is set up to down. The grey arrows in b. and d. indicate an ideal 2:1 decline in TA:DIC.

270 **3.4. Experiment III: Long-term stability of added alkalinity in CO<sub>2</sub> equilibrated approach**

Experiment III was an extension of experiment I, testing for the long-term (up to 90 days) stability of added alkalinity in the two highest treatment levels (abiotic,  $\Delta TA_{2100}$  &  $\Delta TA_{2400}$ ), where for  $\Delta TA_{2400}$  the start  $\Omega_{\text{aragonite}}$  is 13.5, above the critical  $\Omega_{\text{aragonite}}$ , while for  $\Delta TA_{2100}$   $\Omega_{\text{aragonite}}$  is 12.1. Without adding extra particles for the treatment  $\Delta TA_{2100}$  just 50  $\mu\text{mol/kgsw}$  TA were lost after 90 days, while the loss is significantly higher in case of the treatment  $\Delta TA_{2400}$  (-693  $\mu\text{mol/kgsw}$   $\Delta TA_{\text{loss}}$ ), which  
 275 was above the  $\Omega_{\text{aragonite}}$  of about 12.5, identified as being critical for using filtered seawater. While untreated approaches have shown stable values in the first 10 days of runtime, an immediate and persistent decline in  $TA_{\text{final}}$  could be observed for the treatments with added precipitates from previous experiments, functioning as seed material.  $\Delta TA_{2100}$  with particles decreased by 199  $\mu\text{mol/kgsw}$  after 10 days and 757  $\mu\text{mol/kgsw}$  after 90 days, while the  $\Delta TA_{2400}$  treatment dropped by 258  $\mu\text{mol/kgsw}$  after 10 days and 945  $\mu\text{mol/kgsw}$  after 90 days, see Fig. 4a.

280 As in experiment II precipitation at the walls of the reactors were observed. As the treatments here are close or slightly above (Fig. 4) to the supersaturation level where naturally carbonate formation starts, it cannot be ruled out a wall effect caused in the setup with  $\Delta TA_{2400}$  without extra particles the higher loss compared to  $\Delta TA_{2100}$ . Nonetheless experiments in the free water would not face such a wall-effect problem but might be facing a comparable fate due to other surfaces abundant like naturally occurring particles.



285

**Figure 4: Long-term stability of added alkalinity in CO<sub>2</sub> equilibrated approach:** development of alkalinity loss ( $\Delta TA_{\text{loss}}$ ) over time in the two highest alkalinity treatments of experiment I,  $\Delta TA_{2400}$  (red) and  $\Delta TA_{2100}$  (blue), in untreated mode (dotted lines) and with particle addition (solid line) over time. Insert: Development of  $\Omega_{\text{aragonite}}$  in the above treatments. Error bars denote standard deviations of two measures, except for untreated  $\Delta TA_{2100}$  where only one measurement was taken due to technical problems.

### 290 3.5 Experiment IV: Alkalinity addition with brucite

Unlike in the equilibrated and non-equilibrated experiments **I** and **II**, in which an alkaline solution was applied, brucite ( $\text{Mg}(\text{OH})_2$ ) was added as a solid to enhance alkalinity. While  $\text{NaHCO}_3/\text{Na}_2\text{CO}_3$  (equilibrated) and  $\text{NaOH}$  (non-equilibrated) were fully dissolved in the stock solutions after seconds to several minutes,  $\text{Mg}(\text{OH})_2$  dissolved relatively slowly. Due to a comparatively moderate reactivity in seawater, it never reached the point of full dissolution, with the exception of the  $\Delta\text{TA}_{600}$  treatment, which is relatively close to the theoretical solubility of brucite in seawater (determined using PHREEQC, 295 equilibrating seawater with atmospheric conditions) that corresponds to an increase of  $\Delta\text{TA}_{\text{added}}$  of  $\approx 500 \mu\text{mol/kgsw}$  (Fig. 5d). The consequences were transparent to increasingly blurry suspensions, dependent on the added amounts of material. Except for the  $\Delta\text{TA}_{600}$  each reactor had visible residua at the bottom, right after the addition of the solid material. Consequently, the target  $\Delta\text{TA}_{\text{added}}$  steps have not been reached like in the equilibrated and non-equilibrated treatments in experiments **I** and **II**. 300 This also counts for the highest dosage of 1000 mg, corresponding to  $\Delta\text{TA}_{\text{added}}$  of 34,288  $\mu\text{mol/kgsw}$ , see Fig. 5a and d.

Excluding the highest dosage, after the addition of brucite I,  $\text{TA}_{\text{final}}$  reached only 2746  $\mu\text{mol/kgsw}$  ( $\Delta\text{TA}_{\text{net}} = 335 \mu\text{mol/kgsw}$ ) for the target of  $\Delta\text{TA}_{2400}$  at day 0, while for brucite II maximum increase in  $\text{TA}_{\text{final}}$  was achieved at day 1 for  $\Delta\text{TA}_{600}$ . After 1 day of runtime no treatment achieved the target  $\text{TA}_{\text{final}}$  values (Fig. 5a). TA collapsed in all reactors below or close to the initial seawater level at day 4 with exception of biotic treatment  $\Delta\text{TA}_{600}$ . The decline of TA occurred in the form of a ‘runaway precipitation’ as labelled by Moras et al. (2021), meaning carbonate formation causes lower TA-levels than the initial values. 305 This process led to lower  $\text{TA}_{\text{final}}$  values with higher amounts of added brucite at the end of the experiments.  $\Omega_{\text{aragonite}}$  was enhanced moderately up to a maximum of 8.4 in the bulk solution in the abiotic  $\Delta\text{TA}_{2400}$  reactor at day 0, then increased to 11.5 after day 1, and finally declined to relative stable values of 6.8-8.3 after 4 days. pH-values also just experienced a slight increase up to 8.5 at day 0, reached values of 8.5-9.0 in regular steps after 1 day and continued rising in the same stable proportions to 8.6-9.1 (also see Fig. 5c.). 310

While brucite I formed aggregates of particles being insoluble for the duration of the experiment, brucite II (a commercial product for industrial use optimized) did not form aggregates and dissolved more efficiently, leading to higher  $\text{TA}_{\text{final}}$ -levels at day 0. Comparably to brucite I,  $\Delta\text{TA}_{\text{net}}$  levels for brucite II declined in the following four days well below  $\text{TA}_{\text{initial}}$  for treatments  $> \Delta\text{TA}_{600}$ , declining to  $\text{TA}_{\text{final}} \sim 1200 \mu\text{mol/kgsw}$  for  $\Delta\text{TA}_{1800-2400}$ , while  $\Omega_{\text{aragonite}}$  for the same range consistently reached values 315 of  $\sim 5$ , or lower. Only  $\Delta\text{TA}_{600}$  remained slightly above the initial seawater TA level after 4 days, but also declined significantly compared to day 0. For experiment **IV** all treatments showed the same general trends, independent of treatment (abiotic, biotic) or type of brucite.

The high  $\Delta\text{TA}_{\text{added}}$  approach using 1000 mg brucite (corresponding to a theoretical solid material TA addition of 34288  $\mu\text{mol/kgsw}$ ) reached  $\text{TA}_{\text{final}}$  values above 4000  $\mu\text{mol/kgsw}$  at day 0, an  $\Omega_{\text{aragonite}}$  of 24 and pH-values of 9.4. Immediate 320 precipitation at the base of the bottles was observed. The total  $\text{TA}_{\text{final}}$  increase on day 0, however, is on the same general trend.



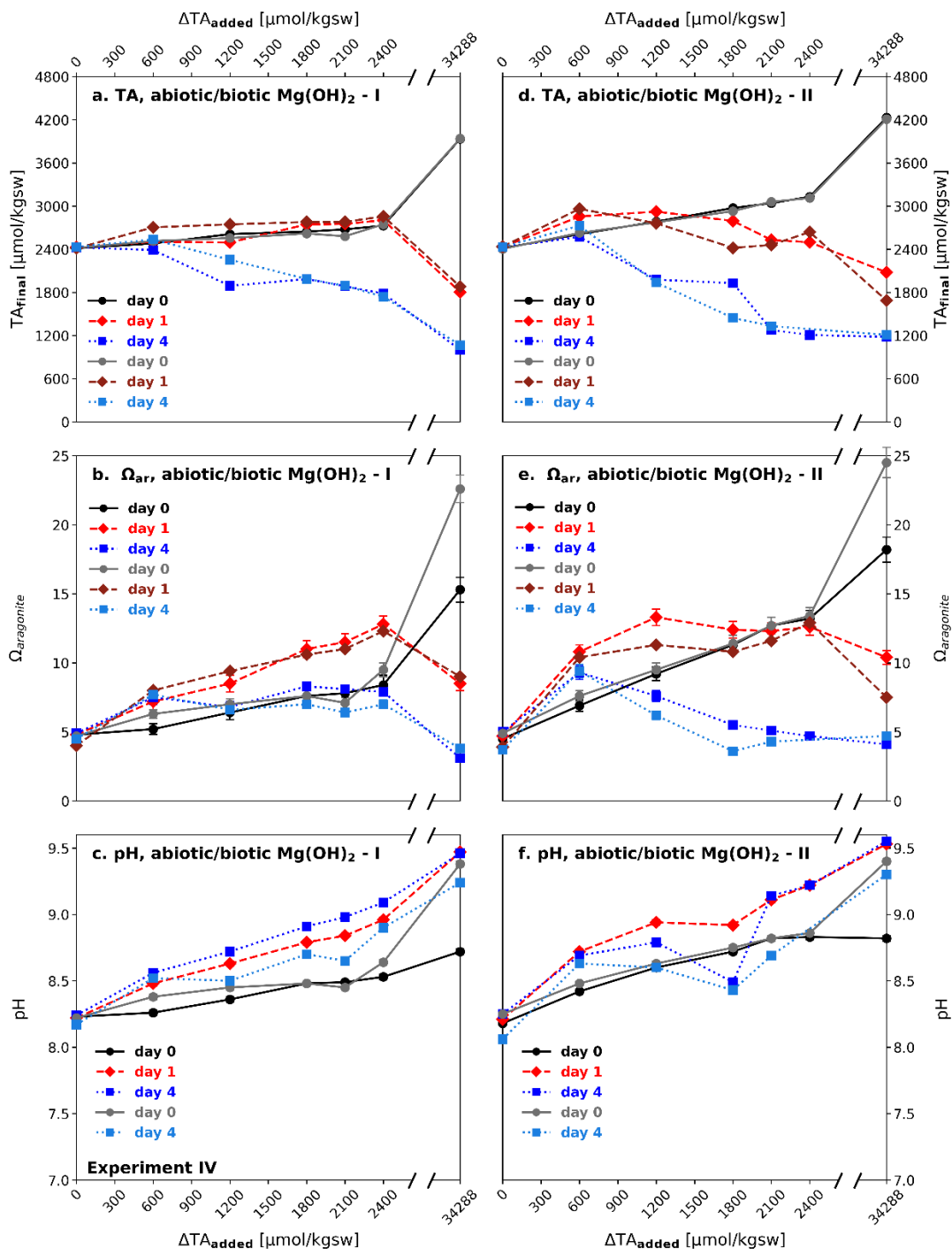
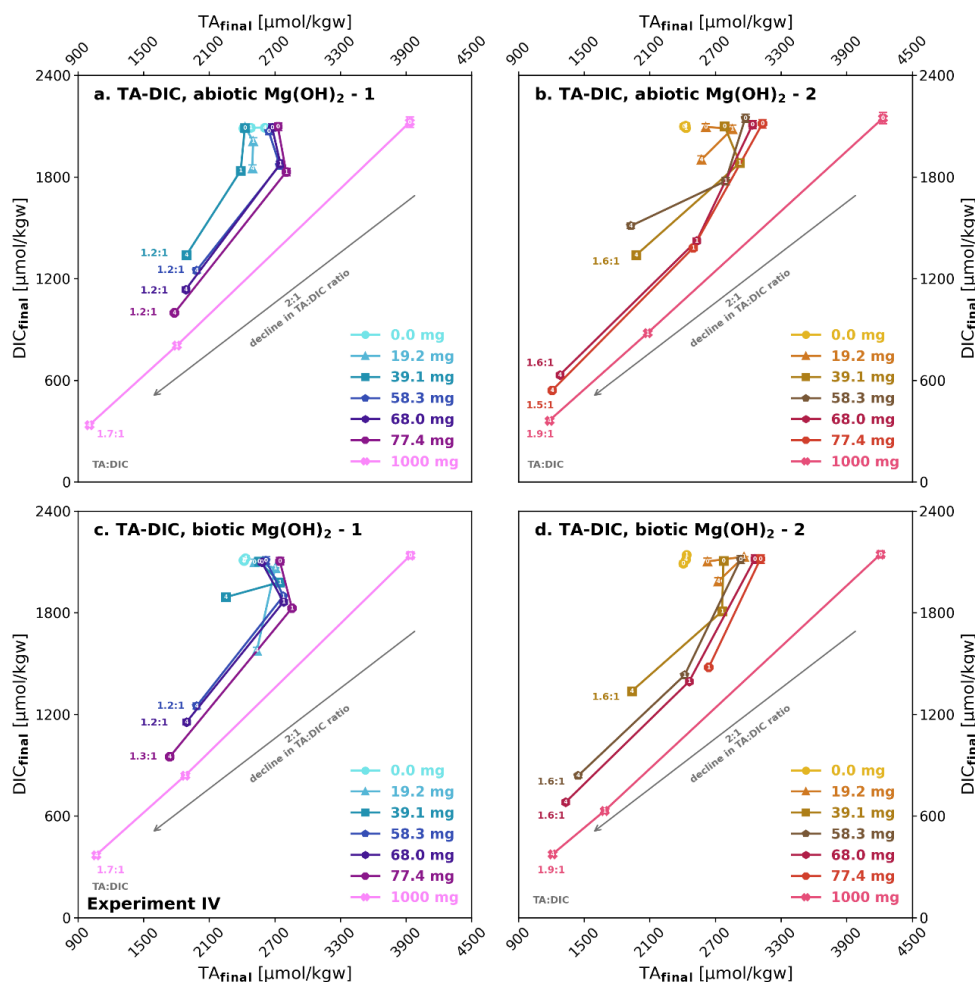


**Figure 5: Dissolution of particulate brucite (types I and II) over time in experiment IV;** (a, d) development of alkalinity ( $TA_{final}$ ), (b, e) aragonite saturation state ( $\Omega_{aragonite}$ ) and (c, f) pH immediately after addition (day 0 – black/grey), 1 day (red) and 4 days after (blue); abiotic treatments – black, red and dark blue graphs, biotic – grey and light blue graphs. Brucite additions range from 19.2 mg ( $\Delta TA_{600}$ ) to 1000 mg ( $\Delta TA_{34,288}$ ). Comparable trends are observed in all treatments, independent of substrate type (brucite I and II) and set-up (abiotic/biotic).

325 **3.6 Experiment IV: TA/DIC evolution brucite**

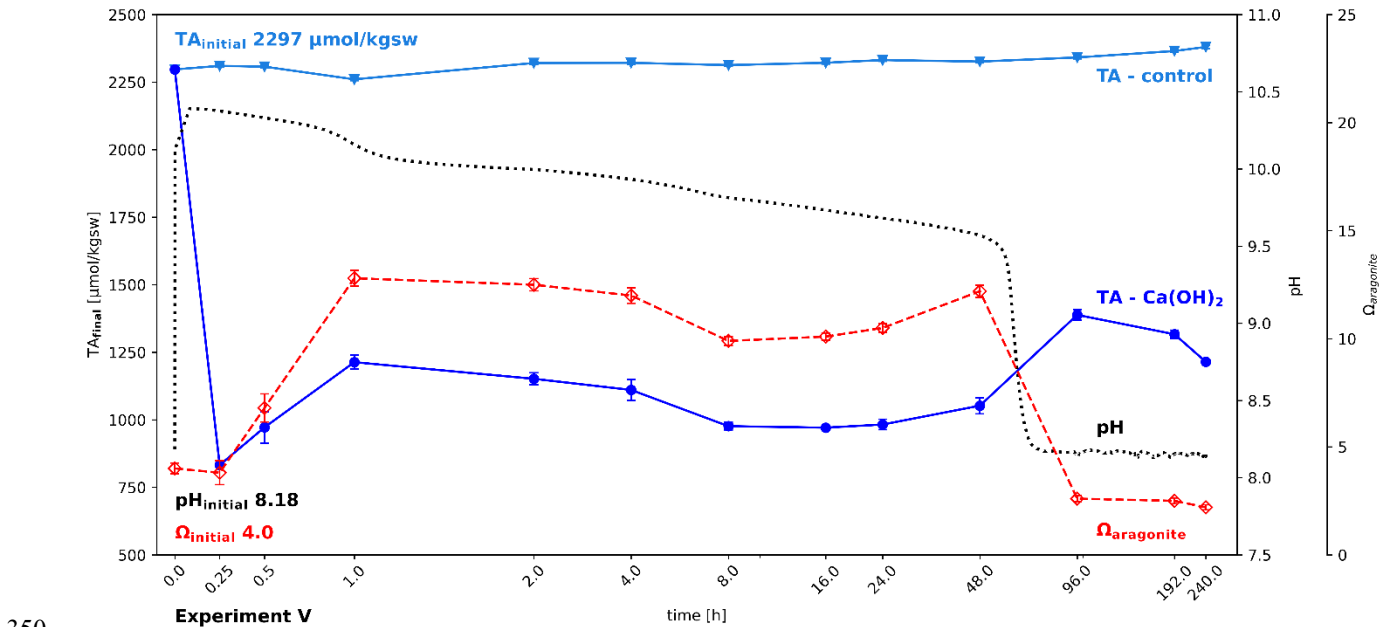
Although for some treatments the TA:DIC development from day 0 to 1 shows some  $TA_{final}$  increase, loss in  $DIC_{final}$  is the general pattern (Fig. 6). Towards day 4 a net loss of  $\Delta TA_{net}$  and  $\Delta DIC_{net}$  can be observed in most treatments. The TA:DIC change ratio thereby differs from that observed in experiment II, where a ratio of 2:1 indicated pure carbonate precipitation, in this case it ranges between 1.2:1 and 1.9:1, clearly showing that in parallel to carbonate precipitation brucite dissolution was still ongoing. In all four treatments there is a tendency of higher TA:DIC change-ratios with higher brucite addition, indicating alkalinity loss due to carbonate precipitation to increase relative to the alkalinity gain due to brucite dissolution. The higher TA:DIC ratios for brucite II (1.6:1 to 1.9:1) compared to brucite I (1.2:1 to 1.7:1) indicate higher carbonate precipitation for the former.



335 **Figure 6: Development of  $TA_{final}$  versus  $DIC_{final}$  during brucite dissolution in experiment IV;** (a, b) abiotic after 0, 1 and 4 days, (c, d) biotic after 0 and 4 days. The days of sampling (0, 1 and 4) are written on top of each data point marker. TA:DIC change ratios for brucite I (1.2:1) and brucite II (1.6:1) are indicating simultaneous precipitation and dissolution, while their difference could be described by their differing dissolution characteristics. The grey arrows indicate an ideal 2:1 decline in TA:DIC.

### 3.7. Experiment V: Alkalinity recovery after mineral precipitation due to CO<sub>2</sub> equilibration with time

This experiment was intended to test for possible recovery of alkalinity after its loss due to mineral precipitation. Addition of 0.66 g/kgsw Ca(OH)<sub>2</sub> and its fast dissolution led to an immediate collapse of alkalinity down to 832 μmol/kgsw within 15 minutes, losing more than half of the initial seawater alkalinity (Fig. 7). At the same time pH increased to above 10.3 and Ω<sub>aragonite</sub> with about 3.8 remained unchanged. In the following hour part of the alkalinity recovered, while Ω<sub>aragonite</sub> further increased to 12.8, accompanied by a steady decline in pH, caused by invasion of CO<sub>2</sub> into the water. After an hour Ω<sub>aragonite</sub> and TA<sub>final</sub> started to decline for the next 48 hours. After that a shift in the carbonate system causes a drastic decline in pH (inflection point at hour 60.4 at pH 9.082) and slight increase in TA<sub>final</sub>, indicating that despite declining Ω<sub>aragonite</sub> some lost alkalinity recovers, which is likely due the redissolution of carbonate forms, not crystallized yet into stable calcite or aragonite. The results show that it is possible to recover, on a time scale of days, some of the lost alkalinity, but despite using a shaking bath to accelerate CO<sub>2</sub> invasion, even after 10 days about half of the initial alkalinity remains lost and the Ω<sub>aragonite</sub> levelled off below the start values.



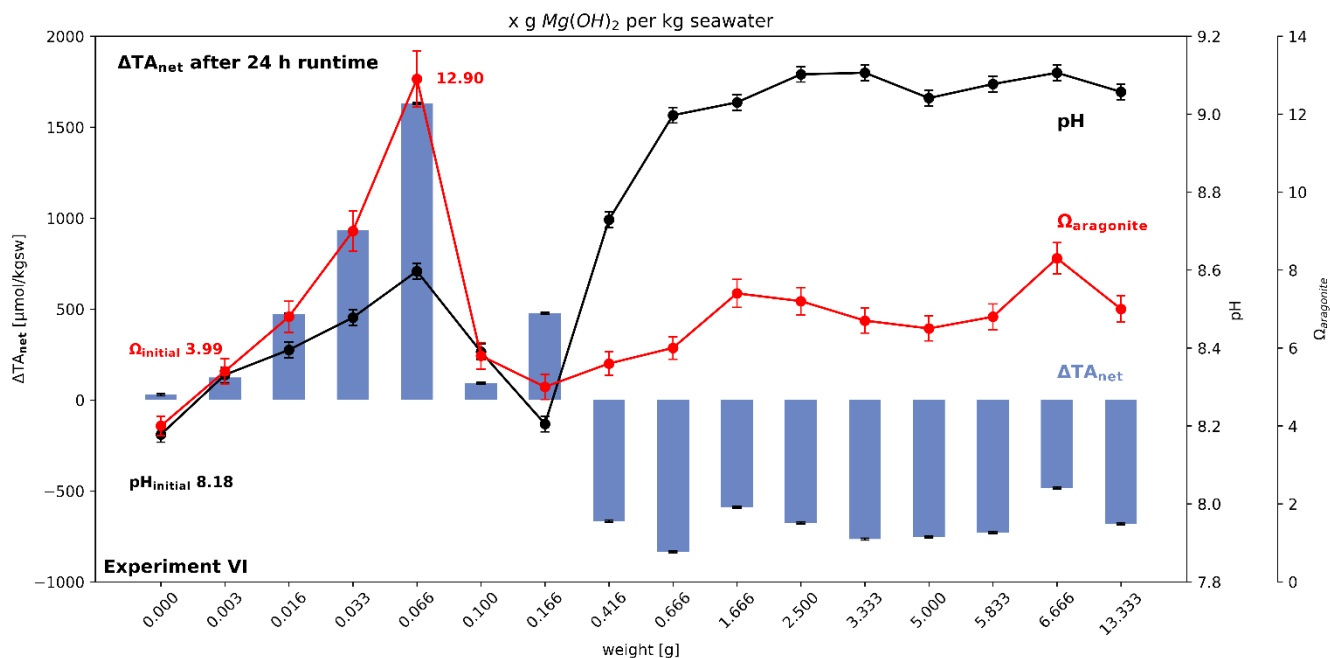
350

**Figure 7: Partial recovery of alkalinity after carbonate precipitation;** Change in alkalinity, pH and Ω<sub>aragonite</sub> after adding 0.66 g Ca(OH)<sub>2</sub> / kgsw to North Sea water in a shaking bath (simulating wave processes to allow accelerated air-water-CO<sub>2</sub>-exchange). Ca(OH)<sub>2</sub> dissolution is so fast, that it is hard to track. While the water gradually equilibrates with the atmosphere, a series of loss and gain of alkalinity can be observed.

355

### 3.8 Experiment VI: Threshold of alkalinity addition to avoid carbonate precipitation

The addition of increasingly larger amounts of  $\text{Mg}(\text{OH})_2$  confirms that the increase in  $\Delta\text{TA}_{\text{added}}$  after 24 hours stops at  $\Omega_{\text{aragonite}}$  close to 12.9 (Fig. 8a). For larger additions net loss of alkalinity was generated, which would subsequently lead to  $\text{CO}_2$  evasion. In the case of  $\text{Ca}(\text{OH})_2$  (Fig. 8b) the net loss switches to alkalinity gain at the highest addition. However, the measured increase in alkalinity ( $\sim 21,000 \mu\text{mol/kgsw}$ ) is less than expected, based on the mineral addition ( $\sim 27,000 \mu\text{mol/kgsw}$ ), suggesting a lower efficiency and therefore higher costs of application. In later experiment, the highest dosage of added  $\text{Ca}(\text{OH})_2$ , shows that still a gain in TA can be achieved. Therefore, two threshold types are demonstrated with this experiment and experiment **IV**: one showing that a threshold level for losing alkalinity after adding a certain amount of solid alkalinity exist, based on material quality, and one gaining at higher levels TA by adding excess solid alkalinity to seawater with a high enough dosage. Interestingly, this effect is not visible using  $\text{Mg}(\text{OH})_2$  at given higher amounts added, suggesting material specific behaviour with different outcome for OAE application. In case of brucite, an important difference to experiment **IV** is the use of a shaking bath, likely making the influence of particle surface processes less effective due enforced advection of water around the particle surfaces. In addition, the shaking conditions causing faster exchange of  $\text{CO}_2$  with the atmosphere do not reflect water bodies directly below the sea surface.



370

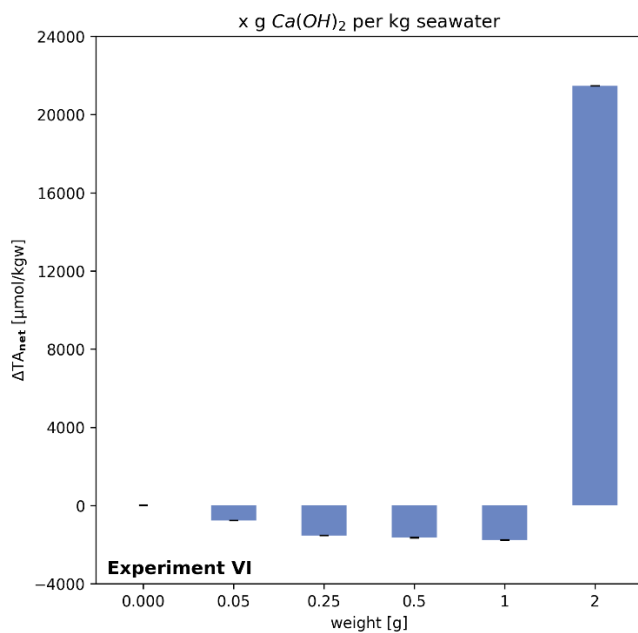


**Figure 8:** Change in alkalinity after adding  $Mg(OH)_2$  or  $Ca(OH)_2$  to North Sea water in a shaking bath (simulating wave processes to allow accelerated air-water- $CO_2$ -exchange). (a) Net loss occurs when alkalinity addition exceeds the critical saturation level of aragonite, while in (b) it is shown, using  $Ca(OH)_2$  that for high added amounts of solid the  $\Delta TA_{net}$ -loss can be turned into a gain. Note for data in 8b no pH values are available for calculation of aragonite saturation levels.

### 375 3.9 SEM images of precipitates

An overview of the shapes and occurrence of calcium carbonate precipitates formed during the loss of alkalinity is provided in Fig. 9. They were derived from experiments IIa ( $\Delta TA_{2400}$ , NaOH – non-CO<sub>2</sub>-equilibrated, Fig. 9a-c) and V ( $\Delta TA_{5400}$ , Ca(OH)<sub>2</sub>, Fig. 9d) after four and ten days, respectively. The precipitates show a variety of symmetrical shapes and structures. These ranged from spheres (or ellipsoids), as the most abundant variant in experiment IIa, to particles with a bi- or multipolar stem (compare to Fig. 10 in Morse et al. (2007)). These stems formed spherical patterns on the tips with elongated crystals, creating porous surfaces. The overall growth patterns showed the development from loosely attached and aligned needle-like crystals to stem-like structures (Fig. 9d) and finally spheres. In general, all sighted samples of experiment IIa and V in which precipitation occurred show the same type and style of precipitation, differing in size and quantity between higher alkalinity and temporal progressed treatments.

385 Fig. 9a gives a general overview, showing all varieties and development stages. Observed average sizes range from 30-50  $\mu\text{m}$ , single spheres in this evolved and high alkalinity treatment ( $\Delta TA_{2400}$ , after 4 days) reached up to 80  $\mu\text{m}$  in diameter. Fig. 9b shows a cluster of partially developed precipitates. Bipolar stems with initial branching structures (I), a broken head of a developed particle (II) from the side, a developed multipolar precipitate with 4-5 heads (III). (II) gives insight of the parallel-aligned crystal growth patterns of the stem as well as the structures branching out. Overall, the “polarity” of each particle

390 seems to be determined in the early stages of formation, single needle-like crystals evolve into bipolar while early-stage crystal branching grows into multipolar shapes. Fig. 9c IV offers a clean-cut cross section through merged components ( $\alpha$ ), a hollow undeveloped stem ( $\beta$ ), and a bipolar branched particle with a failed end which provides insight in the radial crystal growth structure of a head ( $\gamma$ ). Attached to ( $\gamma$ ) is a secondary gypsum crystal which most likely formed during the filtration process, covering the hollow root of the head. To give an overview of the elemental composition of the precipitates, an EDX analysis

395 of ( $\gamma$ ) was added to the supplements (including elemental mapping). Atom percentages reached:  $13.12 \pm 0.80\%$  for Calcium,  $6.15 \pm 0.5\%$  for Magnesium,  $32.63 \pm 4.95\%$  for Carbon and  $46.03 \pm 8.15\%$  for Oxygen, indicating the composition of a Mg-rich calcium carbonate mineral. Fig. 9c V shows an example of an almost closed sphere with the central stem still visible. Particle VI in Fig. 9c represents a transition phase between a dumbbell shape to closed sphere with initial crystal growth bridging the gap between the two heads and starting to overgrow the central stem. Fig. 9d gives a visual impression of the

400 primitive initial needle-like crystals and undeveloped stems of precipitates formed in experiment V. In contrast to the complex forms observed in experiment IIa, primitive initial needle-like crystals and undeveloped stems are dominating here. The precipitation process lasted in experiment IIa several days, while happened in experiment V in a few minutes.

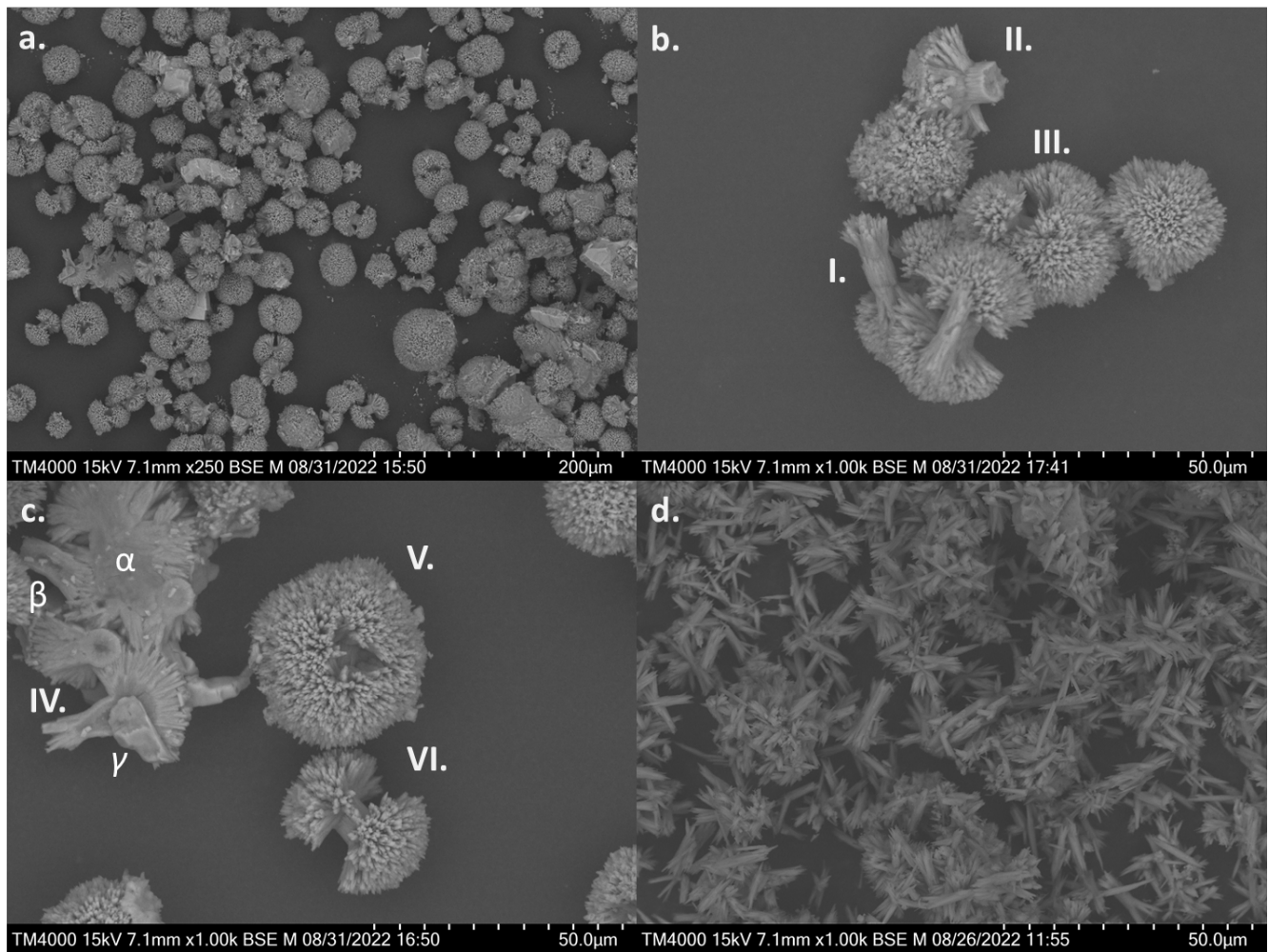


**Figure 9:** Selection of scanning electron microscope images of filtered precipitates from experiments IIa (non-CO<sub>2</sub>-equilibrated – after 405 days) and V (Ca(OH)<sub>2</sub>), a. overview of IIa, b. cluster of precipitates, c. detailed shot of precipitates and cross section through a cluster, showing the internal crystal growth structures, d. overview of precipitates from experiment V (Ca(OH)<sub>2</sub> – after 10 days)

## 4 Discussion

### 410 4.1 General discussion

Results show that the way alkalinity is added to the ocean is crucial to have sustained elevated alkalinity values, and more importantly, to avoid an alkalinity net-loss through carbonate precipitation. Major controlling factors are (i) the type of mineral used, (ii) whether TA is introduced in solid form or as a solution, (iii) in the case of a solution, if it is already enriched with DIC for pCO<sub>2</sub>-equilibrium with the atmosphere or not, and (iv) the presence of biogenic or mineral particles in seawater, affecting 'runaway precipitation' of carbonate (Moras et al., 2021) and associated net loss of TA.

In the approach using alkaline solutions equilibrated with atmospheric CO<sub>2</sub> (experiment I) no  $\Delta TA_{net}$  loss was observed after 4 days, even at high  $\Delta TA_{added}$ . The reason is that the carbonate system (based on  $\Omega(ar)$  of the bulk solution) stayed within boundaries to avoid mineral precipitation for the duration of 4 days. In contrast, application of a solution with elevated alkalinity not equilibrated with atmospheric CO<sub>2</sub> (experiment II; compare Figs. 1 and 2) caused already at the first day a sustained loss of alkalinity, for the high alkalinity addition of 2400  $\mu\text{mol/kgsw}$  (Fig. 2). The reason is that, for the same  $\Delta TA_{added}$ , perturbations of the carbonate system that affect mineral precipitation are much stronger in this non-equilibrated scenario, because alkalinity was added in the pure form of OH<sup>-</sup>, while in the equilibrated experiment alkalinity was added in precalculated ratios of HCO<sub>3</sub><sup>-</sup> and CO<sub>3</sub><sup>2-</sup> to form a water being in equilibrium with the atmosphere. Consequently, treatments with non-equilibrated conditions in experiment II reflect water bodies not being able to equilibrate in time before a loss due critical oversaturation happens, likely to be close below the seawater surface given the slow equilibration with the atmosphere (Jones et al., 2014). This would indicate that usage of reactors to prepare suitable CO<sub>2</sub>-equilibrated alkaline solutions should be considered for large scale OAE (see section below).

Relevant losses for the biotic treatment in experiment II, simulating non-equilibrium conditions, after four days were visible already for treatments with additions > 900  $\mu\text{mol TA/kgsw}$  (Fig. 2). Results of experiment II indicate that a lack of condensation nuclei in the filtered abiotic treatments prevented the start of precipitation at lower TA additions. The difference between biotic and abiotic treatments in experiment II is additional potential seed surface due to particles and plankton >0.2  $\mu\text{m}$  and < 55  $\mu\text{m}$ , which may act as nucleation sites ('seed') for precipitation. In fact, this has resulted in loss of  $\Delta TA_{net}$  at lower  $\Delta TA_{added}$  levels in the biotic treatment. The loss ratio of TA and DIC ( $\Delta TA:\Delta DIC$ ) of 2:1 (Fig. 3b, d) support that the precipitates are carbonates (cf. Fig 9). Comparable observations were made using quartz particles in Moras et al. (2021), because the abundance of potential surface nucleation sites lowers the threshold for alkalinity loss via precipitation.

Notably, once carbonate precipitation is initiated (Fig. 2), TA-loss does not stop at  $\Omega_{aragonite}$  levels of 12.5-13.5 (corresponding to  $\Omega_{calcite}$  levels of 19-20), which were reported (Morse and He, 1993) as threshold levels above which spontaneous carbonate nucleation occurs (in filtered seawater at 25°C and salinity of 35). The threshold for carbonate nucleation is more specific than



spontaneous carbonate formation and growth, e.g. on suitable surface providing optimal surface properties, with lower energy  
440 barriers than nucleation. Once the process of carbonate formation is triggered in this experiment it continues until a certain  
specific thermodynamic equilibrium is reached, which may not have been reached considering the duration of the experiments.  
Experiment **III** demonstrates that the loss of alkalinity can start without particles also at lower than the described critical  
 $\Omega_{\text{aragonite}}$  for filtered seawater if time is longer than 10 days and that the presence of carbonate precipitates from former  
experiments accelerated this process (Fig. 4). Precipitation of minerals at the surface of the walls of the experimental vessel  
445 without adding particles underlines the relevance of surfaces added and their quality as can be seen by the difference in  $\Delta\text{TA}_{\text{net}}$   
for the cases adding carbonate precipitates and not to the bulk water (Fig. 4).

Experiment **IV** differs from experiments **I** to **III**, using alkaline solids  $\text{Mg}(\text{OH})_2$  to produce alkalinity in the seawater while  
providing at the same time a reactive surface area. Carbonate formation and TA loss started in this experiment at  $\Omega_{\text{aragonite}}$  well  
below 12.5 of the bulk solutions. Dissolution-precipitation processes at the surface of the particles happen at the same time  
450 (Figs. 5 and 6), as indicated by the  $\Delta\text{TA}:\Delta\text{DIC}$  change ratios in the bulk water between 1.2:1 and 1.9:1, clearly lower than 2:1  
as expected for carbonate formation alone (compare experiment 2, Fig. 3). The differences in  $\Delta\text{TA}:\Delta\text{DIC}$  change ratios for  
brucite I (1.2:1) and brucite II (1.6:1) for moderate solid  $\Delta\text{TA}_{\text{added}}$  treatments up to  $\Delta\text{TA}_{2400}$  indicate significant product specific  
differences in simultaneous mineral dissolution and carbonate formation characteristics at their surfaces. This result calls for  
detailed product specific evaluation of solid alkaline materials before application, and quality control in case a certain material  
455 might be identified as being useful. In addition, this finding suggests that simple modelling of alkalinity addition based on a  
given mineral type provides no realistic insights into real world ocean alkalinity enhancement applications. In addition, particle  
surface processes on added solid alkaline particles are to be considered. As shown in the equilibrated approach of experiment  
**III** with an added solute alkalinity instead of reactive particles, on longer time scales (here up to 90 days) also the presence of  
potential nucleation sites, in the form of suspended particles or other exposed surfaces, affect the stability of added alkalinity  
460 and hence have to be considered for OAE applications. Importantly, alkalinity loss processes identified in these laboratory  
scale experiments need to be investigated in field trials for further verification and quantification.

#### **4.2 Loss of alkalinity, carbonate formation, temporal stability and potential recovery of alkalinity**

The question of potential recovery of lost alkalinity is even more complicated (experiment **V**, Fig. 7) and is a critical aspect  
for OAE application: If lost alkalinity recovers after a certain time and target TA is reached, then such transient losses could  
465 be accepted. The simple experiment **V** with  $\text{Ca}(\text{OH})_2$ , lasting 10 days, illustrates that alkalinity consumed via carbonate  
formation may partly be released again, here probably facilitated by accelerated ingassing of  $\text{CO}_2$  using a shaking bath (Fig. 7),  
as indicated by the decline in pH after  $\sim 2.5$  days. This shaking bath experiment may not be representative for open ocean  
application, but shows the problem to face, a net loss of TA under certain conditions. Future experiments should gain insights  
under which conditions a temporal loss of alkalinity can be accepted if a net increase would be the result. This was not achieved  
470 in experiment **V**, but could be given different application scenarios or dilution in time (cf. Moras et al., 2021).

In general, amorphous calcium carbonate (ACC) with variable proportion of Mg contents precipitates from water as a precursor prior to the crystallisation of minerals like aragonite or calcite via transformation processes (Rodriguez-Blanco et al., 2017). Direct calcite or aragonite precipitation from water occurs only at high supersaturation levels (Rodriguez-Blanco et al., 2017), which were exceeded in some of the experiments here (cf. Fig. 9) .

475 The precursor ACC leading to an alkalinity loss via nucleation is not stable and can redissolve (Mergelsberg et al., 2020; Brečević and Nielsen, 1989; Clarkson et al., 1992), with reported solubilities more than 100 times larger than for calcite in pure water. Under which conditions ACC precursors formed during OAE can redissolve, to avoid longer-term alkalinity loss, and how fast mixing with untreated water has to be to avoid permanent loss of TA, is - based on few existing data. (c.f. Moras et al., 2021) - difficult to assess for OAE. Further experiments in context of OAE are therefore needed. A good understanding  
480 of mixing rates of treated and untreated water at OAE application sites is therefore critical to avoid permanent TA loss.

The observations from the threshold experiment **VI** (Fig. 8) are making the application more non-trivial, as an excess application of alkaline solids could cause an addition of TA instead of a loss, but with for now unknown consequences for ecosystems due temporal high pH-values above 9.5 for longer time (cf. Fig. 7 using lower doses compared to excess addition in experiment **VI**).

485 In addition, solid particles of different quality, react differently if high application amounts per volume of seawater are used (Fig. 8). In the case of the used  $\text{Ca}(\text{OH})_2$  a gain in  $\Delta\text{TA}_{\text{net}}$  could be observed (Fig. 8b) using high dosages of material (2 g/kgsw versus 1 g/kgsw, which lead to a  $\Delta\text{TA}_{\text{net}}$  loss). For the brucite instead, even adding 13 g/kgsw lead not to a positive change in  $\Delta\text{TA}_{\text{net}}$  after 24 hours. This simple experiment **VI** suggests that  $\Delta\text{TA}_{\text{net}}$ -loss must not be necessarily the case using excess amounts of fast dissolving minerals at the costs of high pH-levels, local critical oversaturation levels, and lower efficiency. As  
490 long as consequences of such excess treatment of seawater are not well enough understood for sustainable OAE management, the combination of results from the experiments **I** to **IV** suggest that adding alkalinity to the ocean should be undertaken such that the rate of increase in  $\Delta\text{TA}_{\text{net}}$  is equal to or less than the rate of re-equilibration of atmospheric  $\text{CO}_2$  to avoid critical oversaturation levels. Such control seems to be difficult to achieve with the direct addition of tested fine solids or highly alkaline liquids not in equilibrium with the atmosphere. It is possible to obtain greater control if a reactor is used to prepare a  
495 pre-equilibrated solution with elevated alkalinity without triggering precipitation ( $\Omega_{\text{aragonite}} < \sim 12.5$ , cf. experiment **I** in Fig. 1b).

Before starting open ocean experiments, detailed model approaches are needed to assess these problems identified here: stability of added alkalinity, possible redissolution of temporary lost alkalinity, and excess application causing a  $\Delta\text{TA}_{\text{net}}$  increase with co-precipitation of carbonates and possibly concerning duration of high pH-values. This in turn needs more  
500 laboratory or mesocosm scale experiments to determine which role particles, present in natural waters, play by lowering the threshold level for potential  $\Delta\text{TA}_{\text{net}}$  loss (cf. experiment **IIa** and **IIb**, abiotic with biotic particles, or Wurgraft et al., 2021) to parameterize models. By now, there are simply not enough reliable data existing to allow for reliable, realistic model

calibration. A serious aspect considering that models are used to assess global and regional potential of OAE, which in turn is used to discuss which CDR-methods are to be considered for future global CDR-schemes.

505 Considering that temporally unstable precursors of carbonate minerals form during the application of OAE, as indicated by experiment **V** (Fig. 7), knowledge about the structure and behaviour of such unstable carbonate species formed is essential for discussing further the application scenarios of OAE. It is relevant to know the fraction and quality of formed unstable carbonate phases which might redissolve under given local and seasonal conditions, as well as application scenarios, because the question of a  $\Delta TA_{\text{net}}$  loss or gain depend on it, and if a  $\Delta TA_{\text{net}}$  loss is only transient for a given acceptable time. Understanding which

510 quality of particle surfaces, and surface area amounts per volume of water, trigger  $\Delta TA_{\text{net}}$ -loss is further to investigate. It is known for a few particles, only. E.g., it is a common laboratory routine to ‘seed’ water with solid carbonates for the initiation of carbonate precipitation (Wurgaft et al., 2021; Morse et al., 2003; DeBoer, 1977). The abundance of suitable surfaces allow carbonate formation and alkalinity loss at lower bulk water saturation levels than used to artificially precipitate carbonates from filtered seawater as shown by Wurgaft et al. (2021) and supported by results from Molnár et al. (2021), and experiment

515 **III** (addition of precipitates from previous experiments). In addition, biotic processes may support carbonate formation at the small scale, via photosynthesis, modulating the local carbonate system via uptake of inorganic carbon (Wolf-Gladrow and Riebesell, 1997). Experiment **II** indicate that ocean-based particles lead to carbonate formation at lower  $\Delta TA_{\text{added}}$  levels compared to filtered water, despite that in this specific seawater only little particles were present.

Because triggered carbonate precipitation aids or boosts further precipitation in seawater, it is in the context of an OAE

520 application scenario essential to understand under which conditions alkalinity loss can be avoided, given the large variety of possible combinations of particles and biota in the world’s ocean. The continued loss of alkalinity well below critical values of  $\Omega_{\text{aragonite}}$  once triggered was labelled ‘runaway precipitation’ by Moras et al. (2021). This aspect needs further understanding based on the few experiments available, as  $\Delta TA_{\text{net}}$ -loss may stop under certain conditions and a possible regain of TA might happen (Fig. 7), which would be a relevant aspect of OAE-management.

525 Specifically, the question about the time window until an amorphous carbonate cluster can redissolve when mixed with untreated seawater is essential for OAE treatment plans and management, considering that sustainable techniques for the application of OAE and monitoring are still missing. Essential global and regional data on stability of TA are still missing and need to be collected at large scale, if OAE should be a practical CDR technology, which is one day emerging from the method idea to a real-world application technology.

530

### 4.3 Consequences for application strategies

Model assessments on the global potential of OAE for long-term CO<sub>2</sub> removal do not consider the risks of alkalinity loss through increased carbonate precipitation (Burt et al., 2021; González and Ilyina, 2016; Ilyina et al., 2013; Kheshgi, 1995; Köhler et al., 2013).

Global modelling studies so far assumed very idealized conditions of OAE, e.g., a spatially and temporally homogenous increase in TA over years or decades. In reality, OAE will likely be achieved via point source release of solid or liquid TA, leading to spatially and temporally much stronger perturbations of the carbonate system, which may in turn trigger carbonate precipitation and  $\Delta\text{TA}_{\text{net}}$  loss. This process might be further facilitated by the presence of particles in seawater, an aspect not considered in models so far.

Results from our study, as well as those from Moras et al. (2021) and Wurgaft et al. (2021) suggest that homogenous or heterogenous nucleation should be avoided to prevent  $\Delta\text{TA}_{\text{net}}$  loss.

The loss of alkalinity in unfiltered water with elevated alkalinity in disequilibrium with the atmosphere after the addition of a solution without particles (Fig. 3, experiment **II**) starts at lower alkalinity additions than in filtered water. The water used in the experiments **I** to **III** is representative for oligotrophic ocean regions, which are low in particle abundance, but it cannot be ruled out that few suspended sediment grains are affecting the results due the close distance to the coast. Wurgaft et al. (2021) showed that particles from river plumes can trigger alkalinity and DIC loss via carbonate precipitation at lower alkalinity levels than used here (~2400  $\mu\text{mol/kgsw}$ ) (Figs. 1 and 2). This observation suggests that without further investigation, application of OAE in such areas should be avoided.

Caserini et al. (2021) modelled ship application of OAE simulating addition of a slurry of Ca(OH)<sub>2</sub>. In their model results, pH levels of 9.2 to 9.5 are reached in open water. Even if these high pH levels would be reached for only a short time (minutes to hours), results here suggest (Figs. 5 to 7) that ship OAE application procedures could result in critical saturation levels, triggering alkalinity loss (cf. experiment **V** and Moras et al. (2021)). Experiment **VI**, however, showed that at the expense of high pH, application of high doses, exceeding the second threshold identified here, results in a  $\Delta\text{TA}_{\text{net}}$  gain, but no loss. But, in that case not all added solid alkalinity is transferred into liquid TA in seawater (Fig. 8: efficiency of 78% after 24 hours for the highest dose).

The addition of non-equilibrated alkaline liquid from a ship would have to be in a way that the saturation state remains below critical thresholds at the site of release. The distribution of the alkaline liquid might be operated via large nets with a network of distributed pressure-nozzles causing small point turbulences for effective mixing of treated water with untreated. Slow point addition rates would increase the ship time needed to deliver a cumulative amount of alkalinity change to the ocean. This would increase the cost, and, where fossil bunker fuel is used, reduce the overall effectiveness of OAE, if ship CO<sub>2</sub>-emissions are not used to produce alkaline solutions added to the ocean. The rate of the ship-based TA-addition would likely be

constrained by the rate of CO<sub>2</sub> resupply to the treated seawater (in general the air-sea gas exchange), and the dilution rate of treated water with untreated.

565 To avoid that added solid particles act as seeds for carbonate precipitation, it may therefore be feasible to add engineered solid particles with sufficiently slow dissolution rate at the particle surface to prevent critical changes in seawater carbonate chemistry, while sink velocity is slow enough to allow for full dissolution close to the sea surface.

An alternative to open ocean addition is the use of reactors to produce equilibrated solutions for the addition into the sea (as shown by experiment I). Reactors for alkalinity production have been proposed for various purposes. For example, Kirchner  
570 et al. (2021) demonstrated on land that it is possible to produce alkaline solutions using limestone and seawater to scrub flue gases of a coal power plant. An alkalinity reactor at the industrial scale for counteracting water acidification in lakes after mining brown coal was built and operated in the Lausitz area, Germany (Koch and Mazur, 2016; LMBV, 2017). The pilot plant to this reactor was able to use solid CaO, Ca(OH)<sub>2</sub> or CaCO<sub>3</sub> and pure CO<sub>2</sub> for alkalinity production.

A further alternative is suggested by experiment I. Na<sub>2</sub>CO<sub>3</sub> and NaHCO<sub>3</sub> dissolve quickly due to their high solubility in  
575 seawater. Results here (Figs. 1 and 3) show that the combination of Na<sub>2</sub>CO<sub>3</sub> and NaHCO<sub>3</sub> to produce a targeted alkaline solution equilibrated with atmospheric conditions give the best outcome for a potentially sustainable alkalinity addition. The application of solid Na<sub>2</sub>CO<sub>3</sub> was already suggested by Kheshgi (1995), but also discarded for global application due to limited natural resources.

It might therefore be worthwhile to study the production of Na<sub>2</sub>CO<sub>3</sub> and NaHCO<sub>3</sub> from CO<sub>2</sub>, NaCl and H<sub>2</sub>O for OAE using  
580 solar thermal energy (Forster, 2014) or possibly as a product of electrochemical approaches (House et al., 2007; Rau et al., 2013). A review on NaHCO<sub>3</sub> production techniques showed that this topic is under-researched (Bonfim-Rocha et al., 2019), opening up the possibility for improvements in terms of cost and energy demand. In addition, new concepts for Na<sub>2</sub>CO<sub>3</sub> production (Forster, 2012, 2014; Wu et al., 2019) provide energetically improved and environmentally friendly production schemes. Such improvements are relevant, in context of needed energy resources.

585 Wu et al. (2019) suggest an energy demand of 5.32 GJ per tonne Na<sub>2</sub>CO<sub>3</sub>, a decrease by 61% compared to standard Solvay process production. Using solar thermal energy for Na<sub>2</sub>CO<sub>3</sub> (Forster, 2014) and NaHCO<sub>3</sub> (Bonfim-Rocha et al., 2019) has the advantage that production is not a burden to the electrical energy grid. Energy costs would be in the range of other discussed CDR approaches, like 4 to 12 GJ/tonne CO<sub>2</sub> for direct air capture (Shayegh et al., 2021; NASEM, 2022), or 3 – 6 GJ/tonne CO<sub>2</sub> for other methods of OAE (Renforth and Henderson, 2017). If the Na-carbonate solids were produced from NaCl solutions  
590 (e.g., through electrochemistry), methods for disposing of the waste HCl acid, or the evolved Cl<sub>2</sub> gas would need to be found (NASEM, 2022). However, HCl could also be a resource to other processes, like the extraction of needed elements for the global energy-transformation from rocks.

#### 595 **4.4 Consequences of alkalinity leakage and impacts of OAE on biota**

Model studies indicate that adding alkalinity to the ocean could remove between 3 and 10 Gt of carbon dioxide per year from the atmosphere, while at the same time counteracting ocean acidification (Feng et al., 2017; Harvey, 2008). However, the potential impact of adding alkaline materials on marine organisms and ecosystems is still largely unknown. Most of the alkalinity enhancement experiments carried out to date have used calcium or sodium hydroxides as alkaline substances  
600 (D'Olivo and McCulloch, 2017; Lenton et al., 2018; Albright et al., 2016; Cripps et al., 2013), and have been tested on a small number of calcifying organisms, like mollusks (Cripps et al., 2013; Waldbusser et al., 2014), corals (Comeau et al., 2012; Albright et al., 2016), and calcifying algae (Gore et al., 2018). In most cases, adding alkaline materials led to enhanced calcification in response to increased calcite and aragonite saturation states. The only in situ experiment in marine waters was carried out in a coral reef, leading to the restoration of calcification of corals that were affected by the decline in carbonate  
605 saturation state caused by acidification (Albright et al., 2016).

Other compounds (like iron, silica or heavy metals) occurring in alkaline rocks that could be added to the water might stimulate or inhibit organism growth, potentially benefiting some organism over others, thereby changing community structure. For instance, a shift towards diatoms and diazotrophic phytoplankton might occur if silica and iron-rich olivine is used as an alkaline agent. On the contrary, the use of alkaline solutions could benefit calcifying plankton, like coccolithophorids (Köhler  
610 et al., 2013; Bach et al., 2019), although diverse adaptations within this group may lead to different responses to OAE (Langer, 2009). Moreover, the addition of technical and natural mineral products may also release trace metals, like nickel in case of olivine dominated dunite (Montserrat et al., 2017).

Overall, the side effects of OAE on organisms, and more importantly on ecosystems, is largely unknown and deserves research at the experimental levels to provide a better knowledge in order to make informed decisions on whether or not alkalinity  
615 enhancement is a feasible mitigation strategy.

#### **5 Conclusion**

From the inorganic geochemical perspective, the amount of potentially formed carbonate phases, their stability (potential re-dissolution), and the subsequent loss of alkalinity after OAE application determines the sustainability of OAE. Understanding these processes and their management will be crucial for the decision-making process regarding OAE application and its  
620 subsequent potential for CO<sub>2</sub> sequestration.

For a given environmental setting, the risk of triggering the loss of alkalinity after OAE is determined by the carbonate saturation state, its temporal evolution and particle surface processes, with the possibility of being steered by the surface area per volume of water as well as the quality of such a surface. To avoid the loss of alkalinity and maximize alkalinity addition, the application of an alkaline solution in CO<sub>2</sub>-equilibrium with the atmosphere and/or solutions with saturation levels that

625 avoid loss of alkalinity is favourable over the application of tested solid materials. Reactor solutions preparing alkaline solutions have been developed for other purposes, like counteracting lake acidification or scrubbing CO<sub>2</sub> from flue gas, and their design could be a blueprint for OAE-reactors.

Formation and redissolution of (temporally) instable carbonate phases are not well understood from the viewpoint of OAE management. This knowledge gap includes natural mixing processes of alkalinity-enhanced water with untreated water, 630 therefore diluting potentially critical conditions in time before permanent secondary precipitation occurs. A pre-application assessment as part of OAE-management, requires therefore detailed information on the hydrodynamics and advection of CO<sub>2</sub> into the water at the site of OAE application.

In addition, a broad spectrum of the effects of duration and degrees of oversaturation levels on permanent carbonate formation (Fig. 7) needs to be studied, including the effect of temperature affecting nucleation kinetics, which was not addressed here. It 635 is likely that in colder waters than tested here, carbonate formation triggered by OAE is delayed via slower kinetics, offering more time for dilution with untreated water. A public database with increasing information on tested materials and gained parameters for OAE application might help in the future to refine OAE assessments on potentials and risks. Such database should include knowledge on the ecosystem response to TA and pH changes, one aspect being understudied.

In conclusion, this study outlined some of the relevant aspects where knowledge on applicability of OAE must be refined 640 before safe and sustainable application boundary conditions and management procedures for OAE can be established.

### **Data availability**

Data will be made available on a publicly available repository upon final publication.

### **Author contributions**

645 JHA conceived the idea for this work. NS, JHA and JT designed the experiments. NS performed the experiments with partial help of JT, CL und JS. JHA wrote the text with the help of all co-authors.

### **Competing interests**

The authors declare that they have no conflict of interest.

### **Acknowledgements**

650 Peggy Bartsch (UHH) and Tom Jäppinen (UHH) are thanked for supporting the preparation and conduction of the experiments. This project has received funding from the European Union’s Horizon 2020 research and innovation programme under grant agreement No. 869357 (project OceanNETs, Ocean-based Negative Emission Technologies - analyzing the feasibility, risks, and co-benefits of ocean-based negative emission technologies for stabilizing the climate) and by the Deutsche Forschungsgemeinschaft (DFG, German Research Foundation) under Germany’s Excellence Strategy – EXC 2037 'CLICCS  
655 - Climate, Climatic Change, and Society' – Project Number: 390683824, contribution to the Center for Earth System Research and Sustainability (CEN) of Universität Hamburg. This is a contribution to the BMBF-project CDRmare RETAKE-J (03F0895J).



## References

- 660 Albright, R., Caldeira, L., Hosfelt, J., Kwiatkowski, L., Maclaren, J. K., Mason, B. M., Nebuchina, Y., Ninokawa, A., Pongratz, J., Ricke, K. L., Rivlin, T., Schneider, K., et al.: Reversal of ocean acidification enhances net coral reef calcification, *Nature*, 531, 362–365, doi: 10.1038/nature17155, 2016.
- Bach, L. T., Gill, S. J., Rickaby, R. E. M., Gore, S., and Renforth, P.: CO<sub>2</sub> Removal With Enhanced Weathering and Ocean Alkalinity Enhancement: Potential Risks and Co-benefits for Marine Pelagic Ecosystems, *Frontiers in Climate*, 1, 1038, doi: 10.3389/fclim.2019.00007, 2019.
- 665 Badocco, D., Pedrini, F., Pastore, A., di Marco, V., Marin, M. G., Bogialli, S., Roverso, M., and Pastore, P.: Use of a simple empirical model for the accurate conversion of the seawater pH value measured with NIST calibration into seawater pH scales, *Talanta*, 225, 122051, doi: 10.1016/j.talanta.2020.122051, 2021.
- Bonfim-Rocha, L., Silva, A. B., Faria, S. H. B. d., Vieira, M. F., and Souza, M. d.: Production of Sodium Bicarbonate from CO<sub>2</sub> Reuse Processes: A Brief Review, *International Journal of Chemical Reactor Engineering*, 0, 1883, doi: 10.1515/ijcre-2018-0318, 2019.
- 670 Brečević, L. and Nielsen, A. E.: Solubility of amorphous calcium carbonate, *Journal of crystal growth*, 98(3), 504–510, doi: 10.1016/0022-0248(89)90168-1, 1989.
- Burt, D. J., Fröb, F., and Ilyina, T.: The Sensitivity of the Marine Carbonate System to Regional Ocean Alkalinity Enhancement, *Frontiers in Climate*, 3, 21, doi: 10.3389/fclim.2021.624075, 2021.
- 675 Caserini, S., Pagano, D., Campo, F., Abbà, A., De Marco, S., Righi, D., Renforth, P., and Grosso, M.: Potential of Maritime Transport for Ocean Liming and Atmospheric CO<sub>2</sub> Removal, *Frontiers in Climate*, 3, doi: 10.3389/fclim.2021.575900, 2021.
- Clarkson, J. R., Price, T. J., and Adams, C. J.: Role of metastable phases in the spontaneous precipitation of calcium carbonate, *Journal of the Chemical Society, Faraday Transactions*, 88(2), 243–249., doi: 10.1039/FT9928800243, 1992.
- Comeau, S., Alliouane, S., and Gattuso, J. P.: Effects of ocean acidification on overwintering juvenile Arctic pteropods *Limacina helicina*, *Marine Ecology Progress Series*, 456, 279–284, doi: 10.3354/meps09696, 2012.
- 680 Cripps, G., Widdicombe, S., Spicer, J. I., and Findlay, H. S.: Biological impacts of enhanced alkalinity in *Carcinus maenas*, *Marine pollution bulletin*, 71, 190–198, doi: 10.1016/j.marpolbul.2013.03.015, 2013.
- D'Olivo, J. P. and McCulloch, M. T.: Response of coral calcification and calcifying fluid composition to thermally induced bleaching stress, *Sci Rep*, 7, 2207, doi: 10.1038/s41598-017-02306-x, 2017.
- 685 DeBoer, R. B.: Influence of seed crystals on the precipitation of calcite and aragonite, *American Journal of Science*, 277(1), 38, doi: 10.2475/ajs.277.1.38, 1977.
- Dickson, A. G.: Standard potential of the reaction:  $\text{AgCl(s)} + 1/2\text{H}_2(\text{g}) = \text{Ag(s)} + \text{HCl(aq)}$ , and the standard acidity constant of the ion  $\text{HSO}_4^-$  in synthetic sea water from 273.15 to 318.15 K, *Chem. Thermodynamics* 22, 113–127, doi: 10.1016/0021-9614(90)90074-z, 1990.
- 690 Dickson, A. G. and Riley, J. P.: The estimation of acid dissociation constants in seawater media from potentiometric titrations with strong base. I. The ionic product of water —  $K_w$ , *Marine Chemistry*, 7, 89–99, doi: 10.1016/0304-4203(79)90001-X, 1979.
- Fakhraee, M., Li, Z., Planavsky, N., and Reinhard, C.: Environmental impacts and carbon capture potential of ocean alkalinity enhancement (preprint), doi: 10.21203/rs.3.rs-1475007/v1, 2022.
- Feng, E. Y., Koeve, W., Keller, D. P., and Oschlies, A.: Model-Based Assessment of the CO<sub>2</sub> Sequestration Potential of Coastal Ocean Alkalinization, *Earth's Future*, 5, 1252–1266, doi: 10.1002/2017ef000659, 2017.
- 695 Forster, M.: Investigations for the environmentally friendly production of Na<sub>2</sub>CO<sub>3</sub> and HCl from exhaust CO<sub>2</sub>, NaCl and H<sub>2</sub>O, *Journal of Cleaner Production*, 23, 195–208, doi: 10.1016/j.jclepro.2011.10.012, 2012.
- Forster, M.: Investigations to convert CO<sub>2</sub>, NaCl and H<sub>2</sub>O into Na<sub>2</sub>CO<sub>3</sub> and HCl by thermal solar energy with high solar efficiency, *Journal of CO<sub>2</sub> Utilization*, 7, 11–18, doi: 10.1016/j.jcou.2014.06.001, 2014.
- 700 Friedlingstein, P., Jones, M. W., O'Sullivan, M., Andrew, R. M., Bakker, D. C. E., Hauck, J., Le Quééré, C., Peters, G. P., Peters, W., Pongratz, J., Sitch, S., Canadell, J. G., et al.: Global Carbon Budget 2021, doi: 10.5194/essd-2021-386, 2021.
- González, M. F. and Ilyina, T.: Impacts of artificial ocean alkalinization on the carbon cycle and climate in Earth system simulations, *Geophysical Research Letters*, 43, 6493–6502, doi: 10.1002/2016gl068576, 2016.
- Gore, S., Renforth, P., and Perkins, R.: The potential environmental response to increasing ocean alkalinity for negative emissions, *Mitigation and Adaptation Strategies for Global Change*, 24, 1191–1211, doi: 10.1007/s11027-018-9830-z, 2018.
- 705 Harvey, L. D. D.: Mitigating the atmospheric CO<sub>2</sub> increase and ocean acidification by adding limestone powder to upwelling regions, *Journal of Geophysical Research*, 113, doi: 10.1029/2007jc004373, 2008.
- House, K. Z., House, C. H., Schrag, D. P., and Aziz, M. J.: Electrochemical acceleration of chemical weathering as an energetically feasible approach to mitigating anthropogenic climate change, *Environmental Science & Technology*, 41(24), 8464–8470., doi: 10.1021/es0701816, 2007.
- 710 Ilyina, T., Six, K. D., Segsneider, J., Maier-Reimer, E., Li, H., and Núñez-Riboni, I.: Global ocean biogeochemistry model HAMOCC: Model architecture and performance as component of the MPI-Earth system model in different CMIP5 experimental realizations, *Journal of Advances in Modeling Earth Systems*, 5, 287–315, doi: 10.1029/2012ms000178, 2013.

- 715 IPCC: Summary for Policymakers. In: *Climate Change 2021: The Physical Science Basis. Contribution of Working Group I to the Sixth Assessment Report of the Intergovernmental Panel on Climate Change*, Cambridge University Press, 2021.
- Jones, D. C., Ito, T., Takano, Y., and Hsu, W.-C.: Spatial and seasonal variability of the air-sea equilibration timescale of carbon dioxide, *Global Biogeochemical Cycles*, 28, 1163-1178, doi: 10.1002/2014gb004813, 2014.
- Kheshgi, H. S.: Sequestering atmospheric carbon dioxide by increasing ocean alkalinity, *Energy*, 20(9), 915-922., doi: 10.1016/0360-5442(95)00035-F 1995.
- 720 Kirchner, J. S., Lettmann, K. A., Schnetger, B., Wolff, J.-O., and Brumsack, H.-J.: Identifying Appropriate Locations for the Accelerated Weathering of Limestone to Reduce CO<sub>2</sub> Emissions, *Minerals*, 11, 1261, doi: 10.3390/min11111261, 2021.
- Koch, C. B. and Mazur, K.: A new technology of pit lake treatment using calcium oxide and carbon dioxide to increase alkalinity, 2016.
- Köhler, P., Abrams, J. F., Völker, C., Hauck, J., and Wolf-Gladrow, D. A.: Geoengineering impact of open ocean dissolution of olivine on atmospheric CO<sub>2</sub>, surface ocean pH and marine biology, *Environmental Research Letters*, 8(1), 014009., doi: 10.1088/1748-9326/8/1/014009, 2013.
- 725 Koishi, A.: Carbonate mineral nucleation pathways, Doctoral dissertation, 194 pp., 2017.
- Langer, G., G. Nehrke, I. Probert, J. Ly, and P. Ziveri: Strain-Specific Responses of *Emiliania Huxleyi* to Changing Seawater Carbonate Chemistry, *Biogeosciences*, 6, 2637-2646, doi: 10.5194/bg-6-2637-2009, 2009.
- Lenton, A., Matear, R. J., Keller, D. P., Scott, V., and Vaughan, N. E.: Assessing carbon dioxide removal through global and regional ocean alkalization under high and low emission pathways, *Earth System Dynamics*, 9, 339-357, doi: 10.5194/esd-9-339-2018, 2018.
- 730 LMBV: In-lake Neutralization of East German Lignite Pit Lakes: Technical History and New Approaches from LMBV, 2017.
- Lueker, T. J., Dickson, A. G., and Keeling, C. D.: Ocean pCO<sub>2</sub> calculated from dissolved inorganic carbon, alkalinity, and equations for K<sub>1</sub> and K<sub>2</sub>: validation based on laboratory measurements of CO<sub>2</sub> in gas and seawater at equilibrium, *Marine chemistry*, 70(1-3), 105-119, doi: 10.1016/S0304-4203(00)00022-0, 2000.
- 735 Mergelsberg, S. T., Yoreo, J. J. d., Miller, Q. R. S., Marc Michel, F., Ulrich, R. N., and Dove, P. M.: Metastable solubility and local structure of amorphous calcium carbonate (ACC), *Geochimica et Cosmochimica Acta*, 289, 196-206, doi: 10.1016/j.gca.2020.06.030, 2020.
- Molnár, Z., Pekker, P., Dódony, L., and Pósfai, M.: Clay minerals affect calcium (magnesium) carbonate precipitation and aging, *Earth and Planetary Science Letters*, 567, 116971, doi: 10.1016/j.epsl.2021.116971, 2021.
- 740 Montserrat, F., Renforth, P., Hartmann, J., Leermakers, M., Knops, P., and Meysman, F. J.: Olivine Dissolution in Seawater: Implications for CO<sub>2</sub> Sequestration through Enhanced Weathering in Coastal Environments, *Environ Sci Technol*, 51, 3960-3972, doi: 10.1021/acs.est.6b05942, 2017.
- Moras, C. A., Bach, L. T., Cyronak, T., Joannes-Boyau, R., and Schulz, K. G.: Ocean Alkalinity Enhancement – Avoiding runaway CaCO<sub>3</sub> precipitation during quick and hydrated lime dissolution, 31, doi: 10.5194/bg-2021-330, 2021.
- 745 Morse, J. W. and He, S.: Influences of T, S and PCO<sub>2</sub> on the pseudo-homogeneous precipitation of CaCO<sub>3</sub> from seawater: implications for whiting formation, *Marine Chemistry*, 41(4), 291-297., doi: 10.1016/0304-4203(93)90261-L, 1993.
- Morse, J. W., Arvidson, R. S., and Lüttge, A.: Calcium Carbonate Formation and Dissolution, *Chemical reviews*, 107, 342-381, doi: 10.1021/cr050358j, 2007.
- Morse, J. W., Gledhill, D. K., and Millero, F. J.: CaCO<sub>3</sub> precipitation kinetics in waters from the great Bahama bank, *Geochimica et Cosmochimica Acta*, 67, 2819-2826, doi: 10.1016/s0016-7037(03)00103-0, 2003.
- 750 NASEM: A Research Strategy for Ocean-based Carbon Dioxide Removal and Sequestration, National Academies of Sciences, Engineering, and Medicine, Washington (DC), 10.17226/26278, 2022.
- Orr, J. C., Epitalon, J.-M., Dickson, A. G., and Gattuso, J.-P.: Routine uncertainty propagation for the marine carbon dioxide system, *Marine Chemistry*, 207, 84-107, doi: 10.1016/j.marchem.2018.10.006, 2018.
- 755 Pierrot, D., Lewis, E., and Wallace, D. W. R.: MS Excel Program Developed for CO<sub>2</sub> System Calculations ORNL/CDIAC-105a (Co2sys\_v2.5) [code], 10.3334/CDIAC/otg.CO2SYS\_XLS\_CDIAC105a, 2006.
- Rau, G. H., Carroll, S. A., Bourcier, W. L., Singleton, M. J., Smith, M. M., and Aines, R. D.: Direct electrolytic dissolution of silicate minerals for air CO<sub>2</sub> mitigation and carbon-negative H<sub>2</sub> production, *Proc Natl Acad Sci U S A*, 110, 10095-10100, doi: 10.1073/pnas.1222358110, 2013.
- 760 Renforth, P. and Henderson, G.: Assessing ocean alkalinity for carbon sequestration, *Reviews of Geophysics*, 55, 636-674, doi: 10.1002/2016rg000533, 2017.
- Rodriguez-Blanco, J. D., Sand, K. K., and Benning, L. G.: ACC and vaterite as intermediates in the solution-based crystallization of CaCO<sub>3</sub>, 2017.
- Sear, R. P.: Nucleation: theory and applications to protein solutions and colloidal suspensions, *Journal of Physics: Condensed Matter*, 19(3), 033101., doi: 10.1088/0953-8984/19/3/033101, 2007.
- 765 Shayegh, S., Bosetti, V., and Tavoni, M.: Future Prospects of Direct Air Capture Technologies: Insights From an Expert Elicitation Survey, *Frontiers in Climate*, 3, doi: 10.3389/fclim.2021.630893, 2021.
- Sun, W., Jayaraman, S., Chen, W., Persson, K. A., and Ceder, G.: Nucleation of metastable aragonite CaCO<sub>3</sub> in seawater, *Proc Natl Acad Sci U S A*, 112, 3199-3204, doi: 10.1073/pnas.1423898112, 2015.

- 770 UNFCCC: Report of the Conference of the Parties to the United Nations Framework Convention on Climate Change (21st Session, 2015: Paris). Retrieved December. Vol. 4. 2015., 2015.
- Uppström, L. R.: The boron/chlorinity ratio of deep-sea water from the Pacific Ocean, *Deep-Sea Research*, 21, 161-162, doi: doi:10.1016/0011-7471(74)90074-6, 1974.
- 775 Waldbusser, G. G., Hales, B., Langdon, C. J., Haley, B. A., Schrader, P., Brunner, E. L., Gray, M. W., Miller, C. A., and Gimenez, I.: Saturation-state sensitivity of marine bivalve larvae to ocean acidification, *Nature Climate Change*, 5, 273-280, doi: 10.1038/nclimate2479, 2014.
- Wolf-Gladrow, D. and Riebesell, U.: Diffusion and reactions in the vicinity of plankton: a refined model for inorganic carbon transport, *Marine Chemistry*, 59(1-2), 17-34, doi: 10.1016/S0304-4203(97)00069-8, 1997.
- Wu, Y., Xie, H., Liu, T., Wang, Y., Wang, F., Gao, X., and Liang, B.: Soda Ash Production with Low Energy Consumption Using Proton Cycled Membrane Electrolysis, *Industrial & Engineering Chemistry Research*, 58, 3450–3458, doi: 10.1021/acs.iecr.8b05371, 2019.
- 780 Wurgaft, E., Wang, Z. A., Churchill, J. H., Dellapenna, T., Song, S., Du, J., Ringham, M. C., Rivlin, T., and Lazar, B.: Particle Triggered Reactions as an Important Mechanism of Alkalinity and Inorganic Carbon Removal in River Plumes, *Geophysical Research Letters*, 48, 277, doi: 10.1029/2021gl093178, 2021.